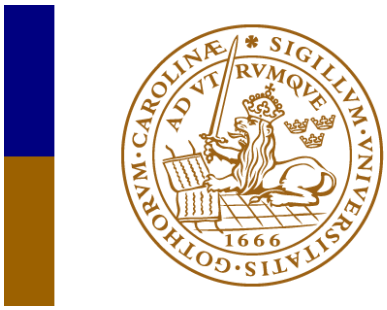

LUND UNIVERSITY
Faculty of Science

Master of Science Thesis

Assessment of radionuclide content in waste barrels using the Canberra In-Situ Object Counting System (ISOCS™)

Marcus Persson

Supervisors:

Karl Östlund[1]
Patrik Konnéus[2]
Sören Mattsson[1]

This work has been performed at Medical Radiation Physics, Department of Translational Medicine, Malmö, Lund University and at Studsvik Nuclear AB, Studsvik, during the spring semester of 2015.

Department of Medical Radiation Physics
Clinical Sciences, Lund
Lund University

[1] Lund University, Department of Translational Medicine, Medical Radiation Physics, Malmö
[2] Studsvik Nuclear AB, Studsvik

Abstract

In order to store radioactive waste its contents need to be known. Determining radioactive waste can be achieved by different means. The most common method is using a detector to measure the gamma photons produced by the radionuclides in the waste. A widely used method is Segmented Gamma Scanning, in which the waste package is rotated in front of a detector and then raised to the next vertical segment etc. until the top of the package is reached. Commercially available waste assay systems from Canberra, ISOCS™, and ORTEC®, ISOTOPIC, exist in which the geometry of the measurement can be modelled in its entirety. Studies are inconclusive as to which accuracy can be achieved.

This work aimed to determine how well Canberra's ISOCS™ could estimate the activity content in a waste barrel with different radionuclide content and waste matrices and to estimate the accuracy of this estimated activity. Also if a NaI(Tl) detector could be used to gain additional information about the measured geometry.

Three different measurement setups were performed at Studsvik Nuclear AB. In setup 1 liquid sources of ^{111}In and ^{131}I and a point source of ^{134}Cs were measured placed in the radial centre as well as in the radial periphery of a barrel filled with water. Homogeneous activity distributions of ^{111}In and ^{131}I were also measured. In setup 2 point sources of ^{57}Co, ^{60}Co, ^{133}Ba and ^{137}Cs were measured in the radial centre and the radial periphery of a barrel filled with water. All point sources were also measured at a different vertical position in the barrel. ^{57}Co and ^{133}Ba were measured individually. In setup 3 a cylindrical liquid source of ^{18}F were measured in the radial centre and radial periphery of a barrel filled with water and homogeneously distributed in the water.

The conclusion is that ISOCS™ can estimate the activity well when the correspondence between the modelled and measured geometry is very good, e.g. sources free in air or homogeneous activity distributions. When the matrices are more complex the correspondence is worse but whether this is due to the software being sensitive for mismatches between the model and reality or because of uncertainties in the experimental setup or a combination of both is not clear. ISOCS™ underestimates the activity content by 60 % for 511 keV when applying a homogeneous activity distribution for a heterogeneous matrix with the source in the centre of the barrel. A NaI(Tl) detector can be used to assess large inhomogeneities in the activity and to apply an accuracy to the activity estimation.

Populärvetenskaplig sammanfattning

Drift av kärnkraftverk och andra kärntekniska anläggningar resulterar i radioaktivt avfall. Att mäta och karakterisera detta avfall finns det ett stort behov av då en tunna med radioaktivt avfall hamnar i olika förvar beroende på hur högaktivt och långlivat innehållet är. Visar det sig att avfallet är tillräckligt lågaktivt kan innehållet friklassas, d.v.s. att hantering/användning av materialet kan ske utan fortsatt kontroll ur strålskyddssynpunkt. För mätning och karakterisering av radioaktivt avfall finns det olika system på marknaden där ett av de vanligast förekommande systemen är ISOCS™ som tillverkas av Canberra, där man i programmet modellerar sin mätuppställning. I detta systemet används en strålningsdetektor, oftast en halvledardetektor av germanium, HPGe (High-Purity Germanium) med hög energiupplösning, som är grundligt karakteriserad av tillverkaren och kalibrerad för olika mätsituationer. Studsvik Nuclear AB utanför Nyköping har två ISOCS™ system som används för just karakterisering av radioaktivt avfall och friklassning av material.

För att ta reda på hur väl ISOCS™ uppskattar aktiviteten i radioaktivt avfall har mätningar med olika strålkällor med känt aktivitetsinnehåll och för olika mätuppställningar utförts. Strålkällorna har varit placerade på olika ställen i en vattenfylld tunna. I andra experiment har radioaktive ämnen spätts ut i vatten för att se hur väl ISOCS™ klarar av denna mätsituation. Till alla mätningar har ytterligare en strålningsdetektor använts i syfte att kunna ta reda på information om den aktuella mätuppställningen som inte går att ta reda på med HPGe-detektorn.

Resultaten visade att ISOCS™ klarar väl av att uppskatta det radioaktiva innehållet i tunnan när aktiviteten är utspädd i vattnet eller när de radioaktiva ämnena var placerade fritt i luft framför detektorn. När ämnena var placerade centralt i tunnan eller i periferin av tunnan så blev överrensstämmelsen sämre. Detta kan bero på systemet eller på grund av att det inte går att uppnå perfekt överrensstämmelse mellan den modellerade mätuppställningen och den praktiska mätuppställningen. Den andra strålningsdetektorn kunde användas för att få reda på mer information om aktivitetsfördelningen i tunnan och öppnar därmed möjlighet till en bättre modellering och förbättrad mätnoggrannhet.

Acknowledgements

I would like to thank my supervisors Karl Östlund, Patrik Konnéus and Sören Mattsson. Karl has been a great support and has continually contributed thoughts and spawned new ideas for the project. In addition to this he has driven me countless kilometres all over our vast country. Patrik has contributed with his expertise and experience with ISOCS™ and has always been available if I needed information or discussion. To Sören for discussions, comments and inputs.

I would also like to thank Studsvik Nuclear AB for the opportunity to do this project, with special thanks to Robert Billnert and Martin Forsström for organising my visits to Studsvik and guiding and supervising me while I was there as well as driving me from Nyköping to the site. Also thanks to Per-Anders Persson for letting me use the system at "R0-A", sometimes with very short notice.

I gratefully thank Jonas Jarneborn for assisting and accompanying me for the second set of measurements. I also direct thanks to Jonas Nilsson for answering my (not always very relevant) questions and providing some useful discussions and inputs.

I direct thanks to the Swedish Radiation Safety Authority for lending me point sources for some of my experiments and to Cecilia Hindorff and the Radionuclide central in Lund for providing me with iodine and indium. I also thank Anders Sandell and the Cyclotron unit in Lund for providing me with excess fluorine from their daily production.

Finally I would like to thank my fellow co-worker Daniel Krona many good discussions and constant companionship.

Table of contents

1 Introduction

There are several different approaches to assess radioactive waste in order to determine if waste material can be cleared or not and they are thoroughly covered in e.g.[1,2]. The most common method of characterizing nuclear waste is non-destructive assay, which is an analysis based on observing ionizing radiation by means of external radiometry in order to estimate the content of one or more radionuclides without affecting the materials physical or chemical form. There are three different methods of performing non-destructive measurements; i.) gamma methods, ii.) neutron methods and iii.) calorimetry, of which the most commonly used are gamma methods[1]. These assay measurement methods relies on detecting gamma photons emitted from the waste materials as part of radioactive decay of the present radionuclides. If so-called "difficult to measure nuclides" are also present, such as beta or alpha emitting nuclides, then they will be determined by the use of "scaling factors" or the use of nuclide vectors[3,4] which correlate the "difficult to measure nuclides" to the more easily measurable gamma emitting nuclides.

There are commercially available systems to characterize nuclear waste where the common systems are ISOCS™[5] from Canberra and ISOTOPIC[6] from ORTEC®. ISOCS™ is a software aiding the user to calculate the radionuclide content of the radioactive waste with precharacterized Canberra detectors. Based on simulation and combined with physical measurements of a reference geometry, the full energy peak efficiency can be calculated for various defined geometries. The ISOTOPIC software utilizes a mixed-radionuclide gamma calibration in conjunction with user specified detector parameters to extrapolate the full energy peak efficiency for the considered geometry. Both systems have been independently verified[7,8].
The commercial systems are versatile in that the specific geometry for the measurement can be specified thus improving accuracy for heterogeneous activity distributions. Still, care needs be taken when using these systems as the standard uncertainty can be as low as 10 % for the best estimates[9] and as high as hundreds of percent for the more complicated matrices[10].

Comparisons between the two systems as well as with other non-commercial systems or with measurements, indicate that ISOCS™ underestimates the activity or activity concentration of radionuclides in different situations[11,12,13,14]. In addition to this there are studies that show very good correspondence in favour of ORTEC®'s software[15, system number 9]. However, there are also studies that show that there is a minimal difference between the two commercial systems[16] and that ISOCS™ show good agreement with other methods[17]. In summary, there are no conclusive results as which to prefer or how well the activity is reproduced.

1.1 Aim

The aim of this master thesis was to:

- Investigate how well Canberra's ISOCS™ could estimate the activity content in a waste barrel with different radionuclide content.
- Investigate how well Canberra's ISOCS™ could estimate the activity content in a waste barrel with different waste matrices.
- Estimate the accuracy for the estimated activity.
- Investigate if an extra NaI(Tl) detector can be used to obtain additional information about the homogeneity of the measured geometry.

2 Background

2.1 Radioactive waste

A number of licensed users of nuclear material and radioactive sources generate radioactive waste; first and foremost nuclear facilities but also hospitals, research laboratories and industries other than the nuclear. In the case of medical use, the vast majority of the radioactive material has a short physical half-life and are thus normally not of concern when it comes to long-term managing of radioactive waste. The Swedish Radiation Safety Authority has made a thorough overview of radioactive waste originating from services in society other than nuclear facilities[18].

Operation and subsequent decommissioning of nuclear facilities inevitably results in a considerable amount of radioactive waste, ranging from spent nuclear reactor fuel to activated concrete or even rubble or dust. This waste needs to be taken care of in a safe way and the measure chosen depends on the physical half-life and activity of the radioactive material involved. Based on IAEA safety standards[19] Sweden has implemented a classification scheme for radioactive waste which determines its destination[20] as shown in Table 1.

Table 1. The classification scheme used for radioactive waste in Sweden[20].

	Destination
Very low level waste, short-lived (VLLW-SL)	Shallow land burial
Low level waste, short-lived (LLW-SL)	Final repository for short-lived Radioactive waste (SFR)
Intermediate level waste, short-lived (ILW-SL)	Final repository for short-lived Radioactive waste (SFR)
Low and intermediate long-lived waste (LILW-LL)	Final repository for long-lived Radioactive waste (SFL)
High level waste (HLW)	Final repository for spent nuclear fuel

The essential difference between the different classes is the dose rate on the surface of the waste package which has to be less than 0.5 mSv/h for short-lived very low level waste, 2 mSv/h for short-lived low level waste and 500 mSv/h for short-lived intermediate level waste. For low and intermediate long-lived waste the package's need to contain significant amounts of long-lived nuclides with half-life longer than 31 years.

As the table indicates, the vast majority of all waste goes to a repository. The existing SFR (Swedish, *Slutförvar För Radioaktivt driftavfall*) consists of rock caverns situated at a depth of 50-140 metres and the planned SFL (Swedish, *Slutförvar För Långlivat radioaktivt avfall*) and final repository will be situated underground as well (as does the central interim storage facility for spent nuclear fuel). This is well in accordance with the preferred strategy for management of all radioactive waste, which is to contain and isolate it from the accessible biosphere in order to protect people and the environment from the harmful effects of ionizing radiation[21]. The safety principles and indeed many principles of radiation protection derive from the recommendations of the ICRP[22].

2.2 Clearance

In addition to the waste classes presented in Table 1, clearance of material is possible which is a practice defined as the "removal of radioactive materials or radioactive objects within authorized practices from any further regulatory control by the regular body" by IAEA[23]. In other words, materials can be cleared for unrestricted use or for disposal as conventional non-radioactive waste, thus enabling a decrease of the amount of radioactive waste ultimately resulting in lower costs. The radiological basis in establishing the level of activity concentration for clearance is that the effective dose to individuals should be less than or equal to 10 μSv in a year[24]. The radionuclide specific clearance levels are implemented in Sweden by the Swedish Radiation Safety Authority[25], and the clearance level for the two most common waste nuclides are presented in Table 2.

Table 2. The clearance levels for the two most common radionuclides in waste.

Radionuclide	**Clearance level** [Bq/kg]
^{60}Co	100
^{137}Cs	1 000

The clearance levels in Table 2 are primarily based upon recommendations from the European Union[26]. The Swedish clearance practice as a whole are covered in detail in a tutorial from the Swedish Nuclear Fuel and Waste Management Co[27].

2.3 Assessment of radioactive waste

There are many different approaches to perform gamma scanning[28], but the most widespread method is Segmented Gamma Scanning, SGS[29]. In SGS the waste package, usually a barrel, is rotated in front of a detector system and at discrete positions a γ-spectrum is obtained. After a complete revolution of the barrel the detector system is raised to the next vertical segment and the procedure is repeated until the top of the barrel is reached. The calculations in SGS generally assume that the matrix and activity distribution for each segment is homogenous. However, in reality the activity is most often not homogeneously distributed in the waste barrels which greatly affects the reliability and accuracy of the reconstructed activities[30]. Extensive work has been done to improve the accuracy of measurements of heterogeneous activity distributions in SGS[31,32,33] as well as for homogeneous distributions [34].

Apart from the SGS there exists several different methods of determining the radioactive content in waste barrels where there are those who use a NaI(Tl) detector[35], a HPGe detector [36] and there are those who use plastic scintillators[37,38,39]. In addition to these there are the commercial systems mentioned in the introduction.

3 Theory

3.1 In Situ Object Counting System - ISOCS™

The Canberra In Situ Object Counting System, abbreviated as ISOCS™, is a system that uses a characterized detector and an individually modelled geometry in order to compute the full-energy peak efficiency. This process begins with creating a mathematical model of the detector and validating this model with real physical measurements using reference point sources. Thereafter this model is used to generate efficiencies at several different points for the detector and from these creating a detector efficiency map. These steps are described in detail below[40].

3.1.1 Mathematical modelling

The ISOCS characterization uses Monte Carlo N-Particle Transport Code, MCNP, which simulates the detectors response to γ-ray sources by imitating the random behaviour of real physical events[41]. A source region is defined and the code simulates the emission of γ-rays with a specified energy distribution and tracking the photon transport through the model, thus taking into account the cross sections for atomic interactions. The deposited energy in the modelled detector are stored in a vector and given as output from the program, representing the energy-response function of the detector. In turn, this can be used to acquire the full-energy efficiency for the modelled source-detector geometry.

3.1.2 The ISOCS characterization process

Developing the ISOCS characterization involves three steps which are briefly described here and in detail below. The first step is developing and validating a model of the detector to be characterized. The second step is generating a vast number of counting efficiency datasets with the simulated detector model in response to point-like sources at a large number of locations around the detector. The third and final step is generating and validating the detector characterization file, containing the relationship between the detector and the point-efficiency data. For more information about this last step, see Appendix A. The characterization process is done by Canberra before the detector is delivered to the customer.

3.1.2.1 Modelling and validating the detector model

In order to develop a model of the detector several different dimensions are needed, such as the length and diameter of the gamma sensitive crystal (most often a High-Purity Germanium detector, HPGe) from Canberra, the dead layer thickness, the detector well and end cap dimensions. In order to define the detectors full-energy peak efficiency response a MCNP model is created by using the above mentioned physical dimensions of the active crystal and all internal structures. Then ISOCS™-based algorithms can be used to calculate the attenuation of the γ-rays traversing the detector holder cup, the detector end cap and the detector dead layer are computed. However, to develop an accurate determination of the physical dimensions it is necessary to determine many of them to a higher degree of accuracy than what is normal in the detector manufacturing process. In reality, the most robust and accurate way to develop a complete model is by comparison with measurements of reference sources.

To improve and validate the detector model, the calculated efficiencies for five different source geometries are compared against corresponding experimentally measured efficiency values, which are determined from point source standards with certified activities of mixed sources of ^{241}Am/^{152}Eu and ^{241}Am/^{137}Cs, respectively. The detector model is validated to these measured reference data by an iterative process using the initial model dimensions as starting

point. To provide optimal agreement between the measured efficiencies and the computed efficiencies the dimensions are adjusted slightly. In the validation process the following five source geometries are used:

I. The ^{241}Am/^{152}Eu source on the detector axis 30 cm from the end cap face.
II. The ^{241}Am/^{152}Eu source at 90°, 2 cm below the end cap face and 32 cm from the axis of the crystal.
III. The ^{241}Am/^{152}Eu source at 135°, at a lateral distance of approximately 22 cm from the axis of the crystal.
IV. The ^{241}Am/^{137}Cs source mounted on a 3 mm thick polymethylmethacrylate (PMMA) disk, positioned 10.4 cm from the detector end cap face.
V. The ^{241}Am/^{137}Cs source mounted on a 3 mm thick polymethylmethacrylate (PMMA) disk, positioned directly on the face on the detector end cap.

The five source geometries above are represented in Figure 1 through Figure 5, respectively.

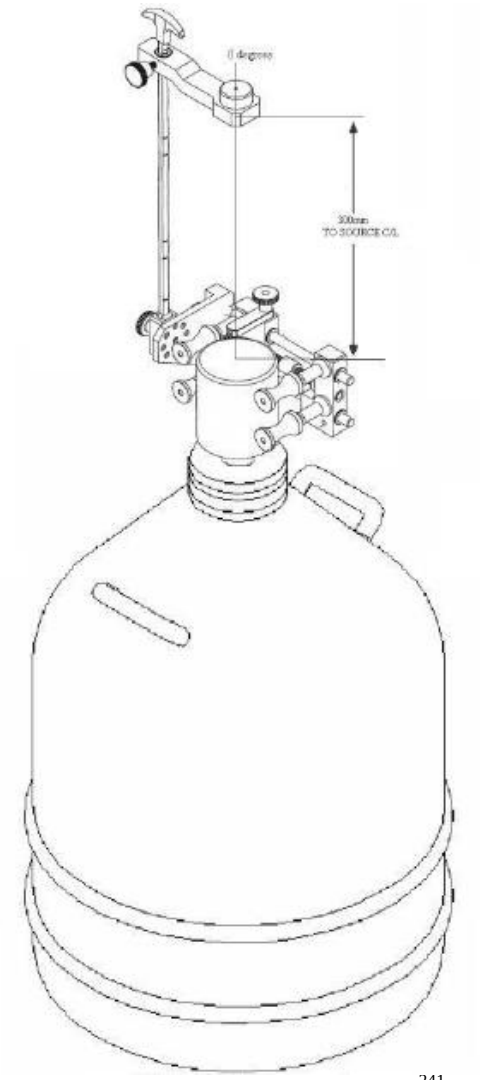

Figure 1. Geometry number 1, with the ^{241}Am/^{152}Eu point source on-axis. The figure depicts an axial measurement on a vertical detector.

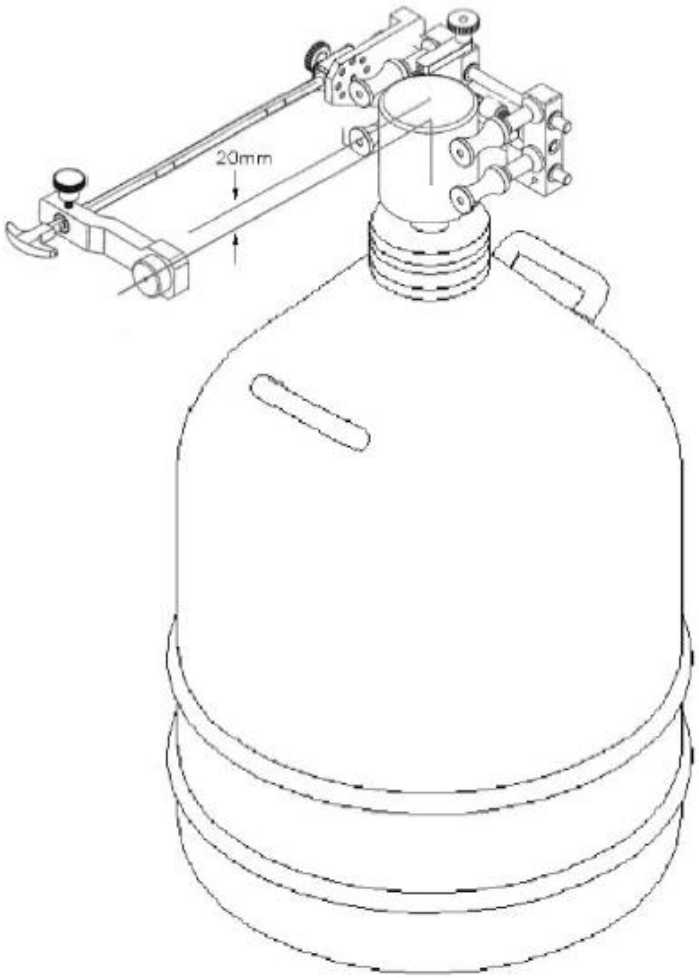

Figure 2. Geometry number 2, with the $^{241}Am/^{152}Eu$ point source at 90°. The figure depicts a lateral measurement on a vertical detector.

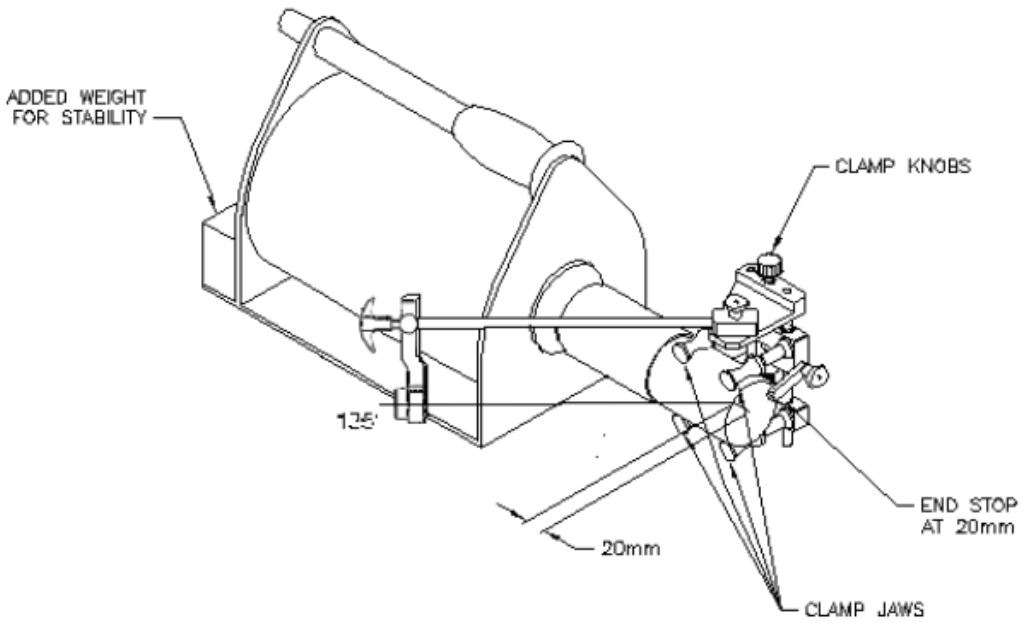

Figure 3. Geometry number 3, with the $^{241}Am/^{152}Eu$ point source at 135°. The figure depicts a lateral measurement.

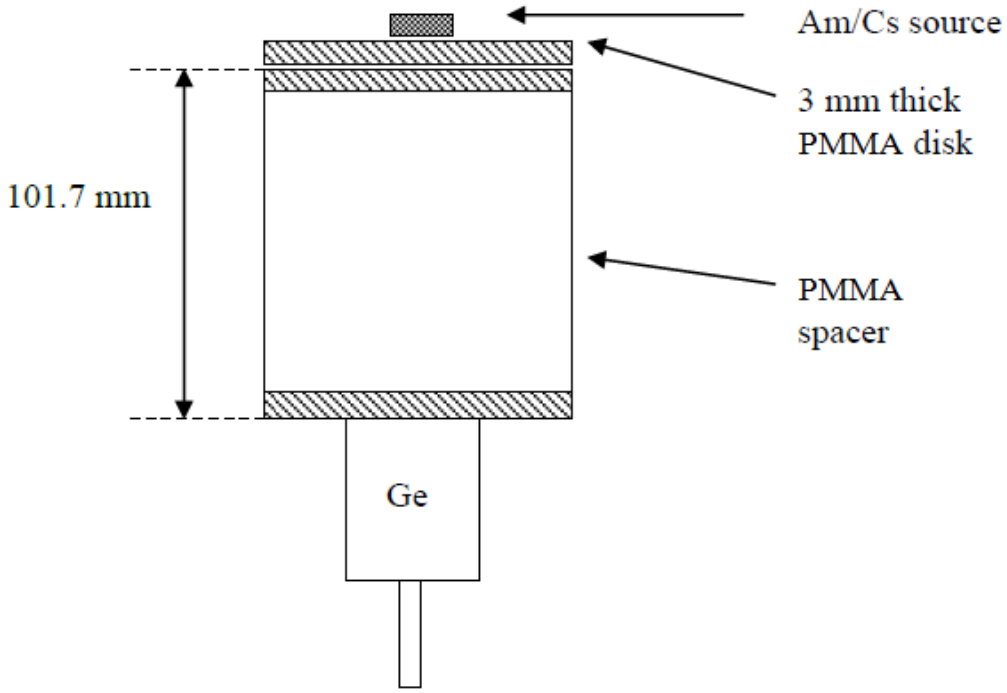

Figure 4. Geometry number 4, with the ^{241}Am/^{137}Cs point source at 104 mm from the detectors end cap.

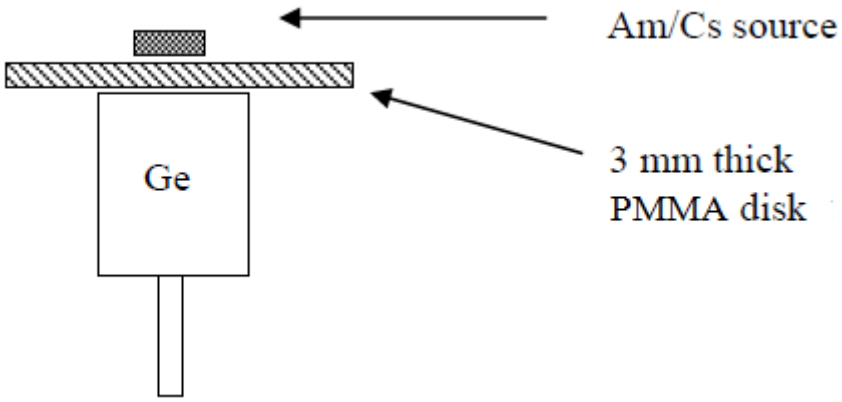

Figure 5. Geometry number 5, with the ^{241}Am/^{137}Cs point source on the detectors end cap.

For the first three geometries the source is mounted in a specially built jig (seen in Figure 1 through Figure 3) which during the source measurements is attached to the detector end cap. This jig provides more accurate and reproducible positioning of the source(s).

For geometries II and III, three measurements are performed where the source is positioned at three equally-spaced azimuthal positions about the detector axis, i.e. at 0°, 120° and 240°. These measurements are performed in order to verify that the crystal is symmetrically mounted inside the end cap. The measured efficiencies from these azimuthal positions are then averaged at each γ-ray energy and used as the measured efficiencies for 90° and 135°.

Geometry IV and V utilises a point source of ^{241}Am and ^{137}Cs mounted on a PMMA disk 3 mm thick. For the measurement of geometry IV the assembly is used with a 10.17 cm high PMMA spacer cylinder placed between it and the detector end cap in order to assure position reproducibility. For the measurement of geometry V the assembly is instead placed directly on the detector end cap.

Both point sources used in these measurements are NIST-traceable sources made by Eckert & Ziegler Isotope Products, Inc. and have an outside capsule measuring 23.5 mm x 10.9 mm x 1.9 mm where the active portion of the source have diameter of 3.3 mm.

3.1.2.2 Generating efficiencies with the validated model

With the model of the detector validated against measured efficiencies it is used to generate triplets of energy, efficiency and uncertainty. Generation of the efficiencies is achieved by a large number of point "source" locations in vacuum at 20 different energies between 10 keV and 7000 keV, where the locations are chosen in order to fill a semi-circular plane which extends from 0° on the detector axis to 180° behind the detector. The locations further extend from the centre of the front face of the detector end cap out to a radius of 500 metres, where the point locations are generated in a specific coordinate system denoted Ln(R)-θ. In this coordinate system R is the radius in centimetres and θ is the angle in degrees. The points are in a grid pattern which spans the whole semi-circular plane and the number of point locations in a diagram of that sort will depend on the size of the crystal and the detectors end cap dimensions.

3.2 Estimation of sensitivity based on point source measurements

Between two extreme values for a point source at its minimum and maximum radial distance, a linear dependency is assumed between the measured activity *k* and the radial position of the source in the barrel. From this a weighting factor can be assigned to the radial position of the point source which can be expressed as an equation as

$$Rel.weight\ (r) = \sum_{i=1}^{N} k \cdot \frac{V_i}{V_{tot}} \qquad (1)$$

where k is the activity for radial position r, V_i is the i:th cylindrical volume element with a radius 5 mm greater than the last element, V_{tot} is the total volume for all elements and N are the number of cylindrical volume elements.

4 Materials and methods

4.1 Summary of experiments

Three different sets of measurements were performed at Studsvik Nuclear AB and they are presented in Table 3.

Table 3. Summary of the performed sets of measurements at Studsvik Nuclear AB.

Setup	Radionuclides used	Matrices
1	^{111}In, ^{131}I and ^{134}Cs	Point sources placed in the radial centre and radial periphery of a barrel. Also homogeneous activity distribution of ^{111}In and ^{131}I.
2	^{57}Co, ^{60}Co, ^{133}Ba and ^{137}Cs	Point sources placed in the radial centre and radial periphery of a barrel. Also single sources and at different vertical position.
3	^{18}F	A point source placed in the radial centre and radial periphery of a barrel. Also homogeneous activity distribution.

In addition to the measurements at Studsvik Nuclear AB, measurements were performed at Medical Radiation Physics in Malmö in order to estimate the geometrical uncertainty as described by the variation in the total number of counts at repeated measurements using a NaI(Tl) detector.

4.2 Overall

All measurements at Studsvik Nuclear AB were performed with the sources placed in a steel barrel with inside height 700 mm, inside diameter 470 mm, wall thickness 0.7 mm and density 7.86 g/cm³ filled with water. In the lid, aluminium rods had been installed in order to place the sources at the desired position, see the left side of Figure 6. A barrel identical to the ones used and the lid with the aluminium rods used in the experiments are presented in Figure 6. For the first two sets of measurement, the barrel was measured in four different directions with 90 degrees intervals, as seen schematically in Figure 7 and Figure 8. The purpose of measuring each of the four sections was to investigate whether the activity content could be reproduced equally well independently of where the source is located in the barrel, due to the possibility to model the source at any place within the barrel. The barrels were also measured while rotating since this is how the barrels normally are measured. In order to observe any difference between different waste matrices, measurements were performed with both homogenous and heterogeneous activity distributions. In section 4.4 all measurements are performed with measurement time 300 seconds except where otherwise noted.

Figure 6. To the left a steel barrel with inside height 700 mm, inside diameter 470 mm and wall thickness 0.7 mm. The image to the rights depicts a lid with aluminium rods used to place the sources at the first two setups.

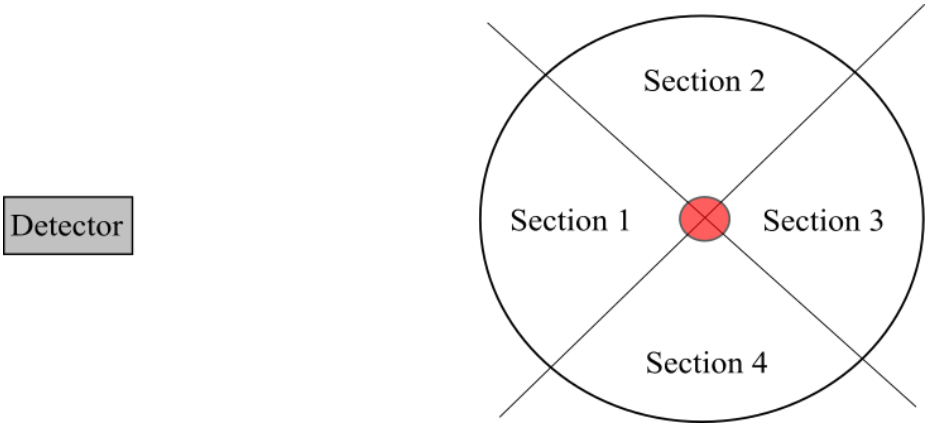

Figure 7. Schematic illustration of the different sections when the measurement geometry is such that the point source (red) is in the radial centre of the drum. Please note that the distances and sizes are not to scale.

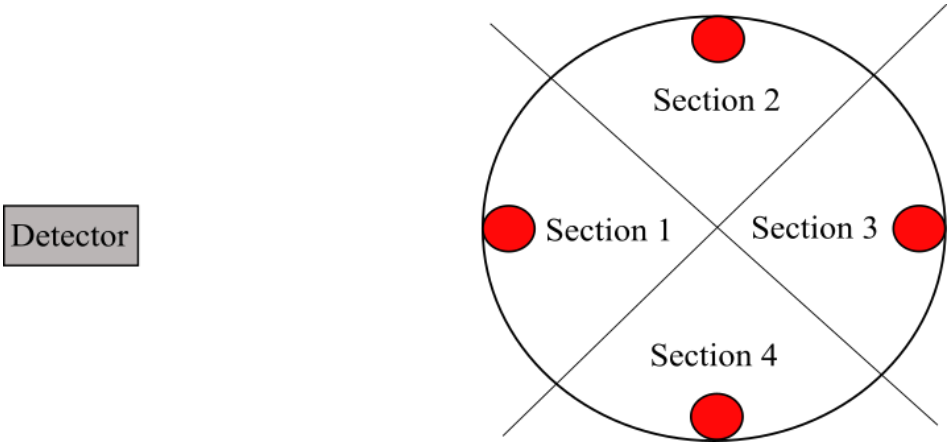

Figure 8. Schematic illustration of the different sections when the measurement geometry is such that the point source (red) is located in the radial periphery of the drum. Please note that the distances and sizes are not to scale.

4.2.1 Detector systems

Studsvik Nuclear AB utilise two different ISOCS™ systems[3] where one is located at a site called “HA” which deals primarily with final conditioning measurements of waste parcels in the form of barrels of varying size with unknown nuclide and activity content. The other is located at a site called “R0-A” which primarily measures parcels and objects of varying type for clearance.

4.2.1.2 HA

The system at “HA” consist of a Canberra p-type coaxial High-Purity Germanium detector with a relative efficiency of 45 %, model number GC4519 and S/N B04089. Surrounding the detector are lead collimators which limit the detector field of view to 2π. The detector was connected to a preamplifier and a cryostat, both from Canberra with model numbers 2002C and 7600-RDC-4, respectively. The detector was placed at a distance of 226 cm from the reference plane of the barrels (see Figure B1and Figure B2 in Appendix B) used when centred on the rotation plate. The central axis of the detector was located at height 68.3 cm from the floor. For the barrels used, the offset between the source reference point (R in Figure 15 and Figure B1, Figure B2 and Figure B3 in Appendix B) and the detector aiming point (A in Figure 15 and Figure B1, Figure B2 and Figure B3 in Appendix B) was 30.7 cm as was the offset between the detector reference point (centre of the detector end cap, D in Figure 15 and Figure B1, Figure B2 and Figure B3 in Appendix B) and the source reference point. The detector system is presented in Figure 9 and a schematic of “HA” are illustrated in Figure 10.

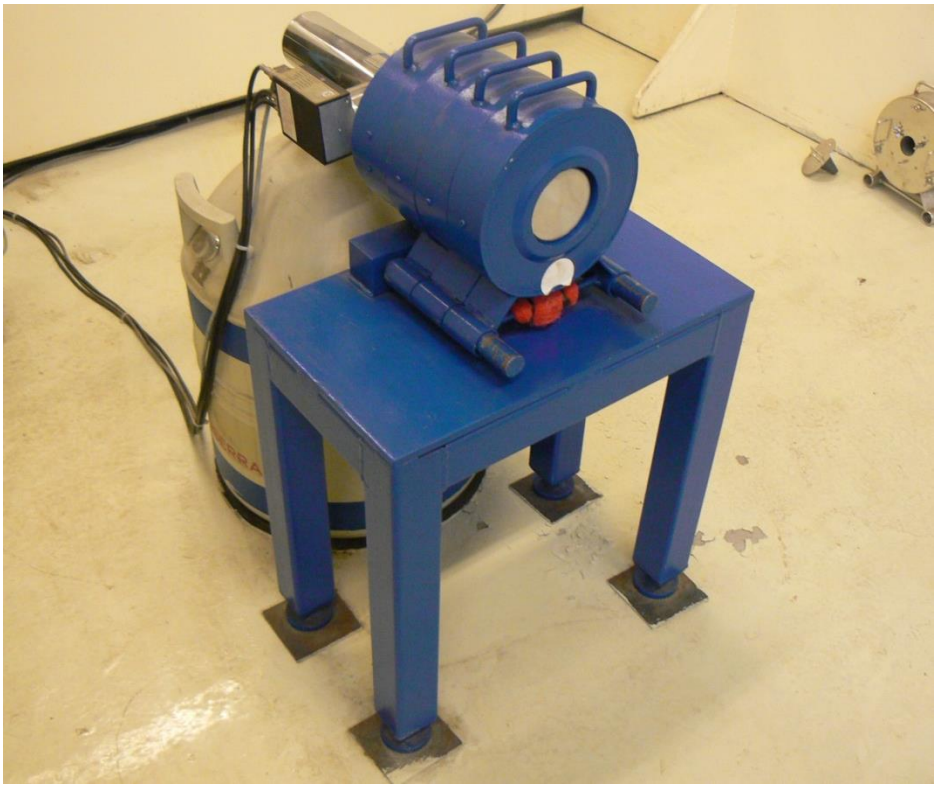

Figure 9. The system setup at “HA”, with the p-type HPGe detector with relative efficiency 45 % complete with cryostat and lead collimation.

[3] Canberra Industries Inc.

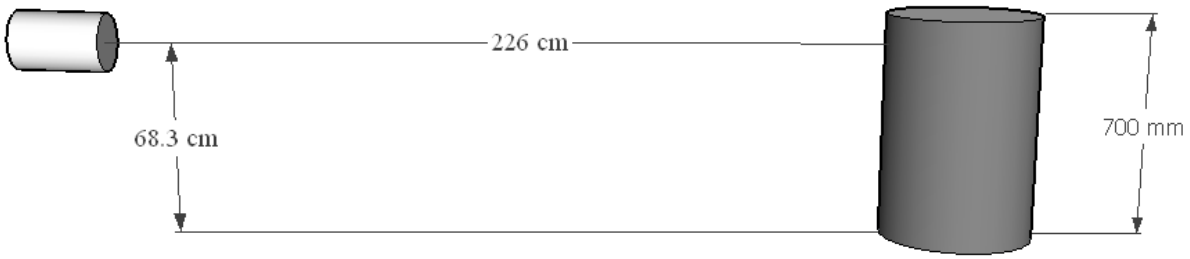

Figure 10. A schematic drawing of the system setup at "HA" where the barrel is identical to the ones used in this work. Please note that the distances and sizes are not to scale.

4.2.1.2 R0-A

The system at "R0-A" consist of a Canberra p-type Broad Energy Germanium (BEGE) detector with a relative efficiency of 48 %, model number BE5030 and S/N b00009. The detector was collimated with lead similar as the aforementioned HA-system resulting in a 2π detector field of view. The detector was connected to a Canberra preamplifier 2002C and a Canberra cryostat 7935-7F-RDC-4. The detector was placed at a distance of 126 cm from the reference plane of the barrels (see Figure B1and Figure B2 in Appendix B) used if centred on the rotation table, which had an elevation of 49 cm from the floor. The central axis of the detector is located at height 95.6 cm from the floor. For the barrels used the offset between the source reference point (R in Figure 15 and Figure B1, Figure B2 and Figure B3 in Appendix B) and the detector aiming point (A in Figure 15 and Figure B1, Figure B2 and Figure B3 in Appendix B) was 10.0 cm and the offset between the detector reference point (centre of the detector end cap, D in Figure 15 and Figure B1, Figure B2 and Figure B3 in Appendix B) and the source reference point was also 10.0 cm. The detector system is presented in Figure 11 and is located in a room with walls and door made of low-background steel, which is often referred to as a low background room or low background facility. A schematic of "R0-A" are illustrated in Figure 12.

Figure 11. The system setup at "R0-A", with the p-type HPGe detector with relative efficiency 48 % complete with cryostat and lead collimation.

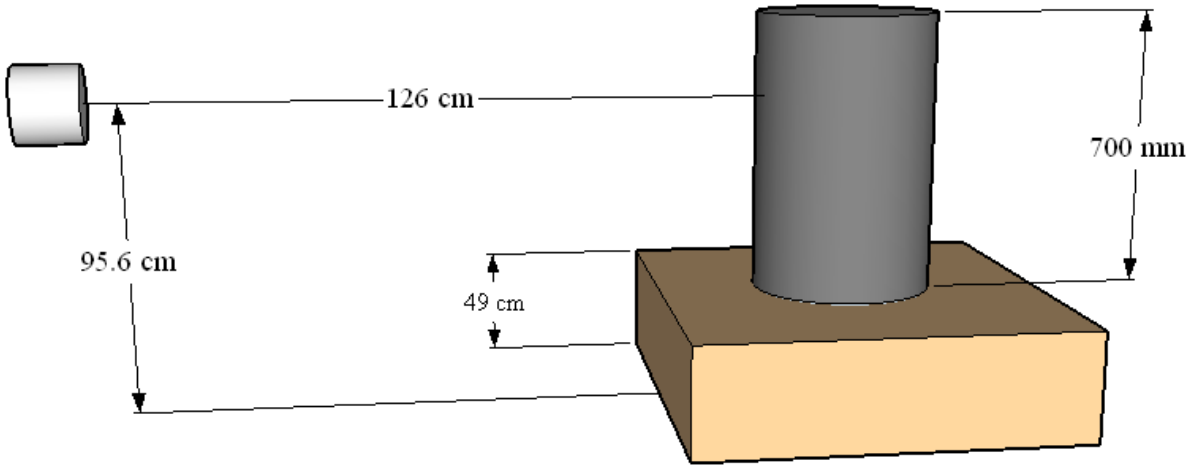

Figure 12. A schematic drawing of the system setup at "R0-A" where the barrel is identical to the ones used in this work. Please note that the distances and sizes are not to scale.

4.2.1.3 NaI(Tl) detector

The portable NaI(Tl)-system used consisted of a Ø 76.2 mm x 76.2 mm NaI(Tl) detector manufactured by Saint-Gobain Crystals with an integrally mounted Bicron® PM-tube, model number 3M3/3 and S/N 60004-02515-I. Connected to the PM-tube was an ORTEC® digiBASE™ which is a unit that contains preamplifier, amplifier, analogue-to-digital converter and multichannel analyser as well as a high voltage supply[42]. The detector with its integrated PM-tube and digiBASE™ were all encapsulated in a protective aluminium cylinder with wall thickness 5 mm and front end cap thickness 2 mm and the detector system is presented in Figure 13. In all measurements performed in this work the applied voltage to this detector was + 770 V and no collimation were used for the detector. At "HA" the detector was placed at height 61 cm from the centre of the detector to the floor and at a distance of 40 cm from the end cap to the surface of the barrel. The detector was placed facing the rotational centre of the barrel in the centre of a section. At "R0-A" the NaI(Tl) detector was placed at height 72 cm from the centre of the detector to the floor except where noted and at a distance of 100 cm between the end cap and the surface of the barrel. The detector was placed facing the rotational centre of the barrel in the centre of a section.

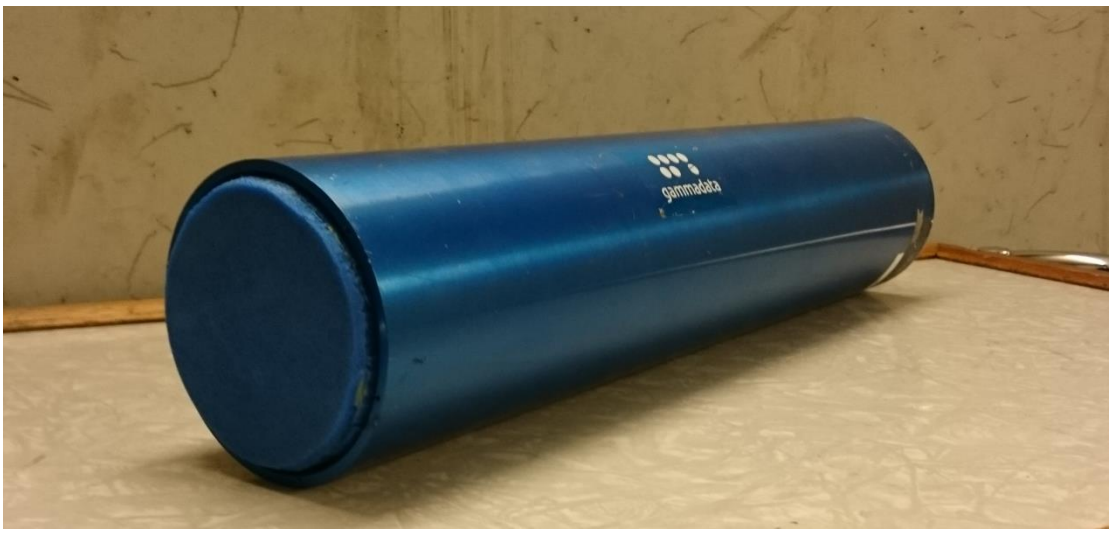

Figure 13. NaI(Tl) detector in aluminium rod with the front end cap removed.

4.2.2 Radiation sources

Different sources of different radionuclides were used for the experiments and their characteristics are summarised in Table 4 with energies, physical half-lives and photon yields according to IAEA[43]. The activities of the sources are specified in the corresponding experiment.

Table 4. Radionuclides used during the experiments, their γ-energies with corresponding yield and type of source. In the column "Physical half-life" min = minutes, d = days and y = years.

Isotope	**Physical half-life**	**Photon energy [**keV]	**Yield** [%]	**Type of source**
^{18}F	109.77 min	511	193.5	Liquid cylinder source in glass vial
^{57}Co	271.74 d	122.1 136.5	85.6 10.7	Sealed point source
^{60}Co	5.271 y	1173 1332	99.9 100	Sealed point source
^{111}In	2.805 d	171.3 245.4	90.8 94.1	Liquid cylinder source in glass vial
^{131}I	8.025 d	80.19 284.3 364.5 637.0 722.9	2.62 6.13 81.6 7.16 1.77	Liquid cylinder source in plastic vial
^{133}Ba	10.55 y	81.00 276.4 302.9 356.0 383.8	32.9 7.17 18.3 62.1 8.95	Sealed point source
^{134}Cs	2.065 y	563.2 569.3 604.7 802.0 1168 1365	8.34 15.4 97.6 8.67 1.79 3.02	Sealed point source
^{137}Cs	30.08 y	661.7	85.1	Sealed point source

All sealed point sources in Table 4 are from Eckert & Ziegler Isotope Products, Inc. and are in accordance with Figure 14. Not seen in the figure is the aluminized mylar with thickness 0.254 mm that covers the active area.

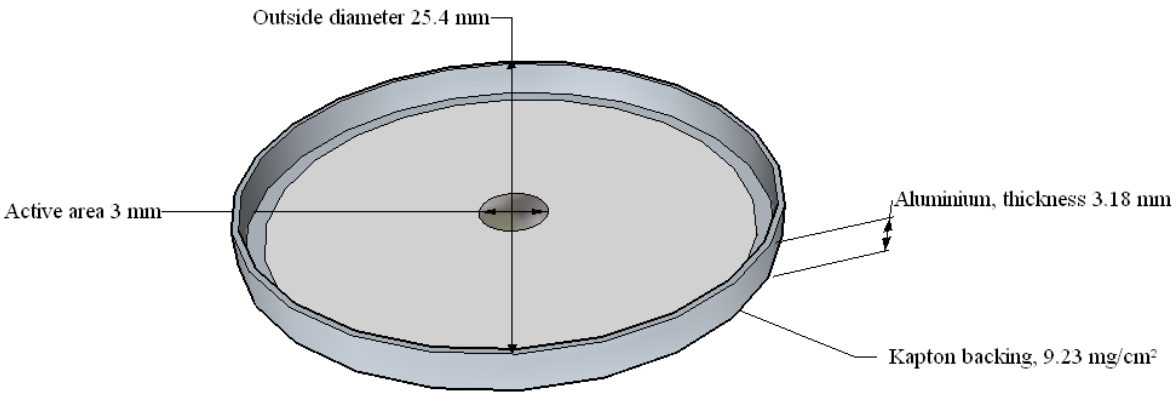

Figure 14. A graphic illustration of the point sources used in the measurements, lacking the 0.254 mm thick layer of aluminized mylar that covers the active area.

4.3 Modelling the measurement geometries

To perform the required efficiency calibration in order to estimate the activity content in the barrels three predefined geometries were used; the "Simple Cylinder", "Complex Cylinder" and "Sphere" templates. How to define the specific dimensions in the templates are described in the ISOCS™ manual and are also found in Appendix B. The user has to be certain of all densities of the model and activity concentration when using this tool since the accuracy of the efficiency calibration is dependent upon correct input. An example of a typical template is given in Figure 15 where the illustration for the "Sphere" template is shown. For further details see Appendix B.

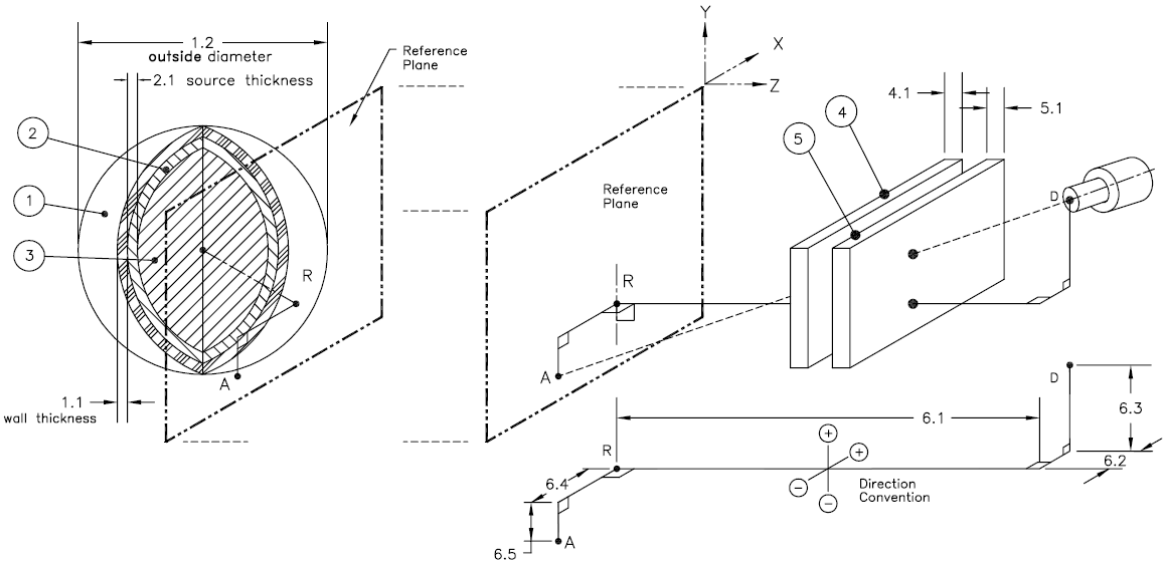

Figure 15. An example of a typical template utilised in ISOCS™ for modelling the measurement geometry. The template shown is the "Sphere" template.

4.4 Experiments

4.4.1 Measurements on two different matrices using ^{111}In, ^{131}I and ^{134}Cs

Two different setups were used; one with heterogeneous activity distribution and the other with homogenous activity distribution. In both barrels two plastic bags were applied on the inside to avoid radionuclide attachment to the inside of the barrel. The radionuclides used were ^{111}In, ^{131}I and ^{134}Cs (see Table 4) and where the activity was put in two vials each of ^{111}In and ^{131}I. The measurements were decay corrected and therefore a reference time for their activities was set to 13:50 19th of February 2015 which was the first day of measurement. The same reference time is used for the ^{134}Cs source. The activities are presented in Table 5.

Table 5. The activities of the sources used for the first set of measurements with reference time 13:50, February 19, 2015. The uncertainty for the vials activities are based on the precision from the manufacturer of the ionization chamber in which their activities were measured[44]. The uncertainty for the point source activity is the total uncertainty at the 99 % confidence level given by the manufacturer Eckert & Ziegler Isotope Products, Inc.

Isotope	**Source**	**Activity** [MBq]
^{111}In	Vial 1	7.85 ± 0.2
	Vial 2	10.5 ± 0.2
^{131}I	Vial 3	8.45 ± 0.2
	Vial 4	13.4 ± 0.2
^{134}Cs	Point source	2.52 ± 3%

Before the sources were applied in the barrels, a measurement was performed free in air on vial 2 of ^{111}In, vial 3 of ^{131}I and the point source of ^{134}Cs in order to determine how well ISOCS™ could estimate the activity in the simplest reference geometry situation. The sources were placed on a steel table with height 56 cm in the centre of the rotating plate at "HA" and measured during 600 seconds. The geometry modelled for this measurement were created from the "Sphere" template (see Figure 15 or Figure B3 in Appendix B) with the source made of PMMA, ρ=1.2 g/cm³, with relative concentration 1.0, diameter 35 mm and source shell thickness 0.2 mm also made of PMMA.

The barrel with heterogeneous activity distribution was filled with 107 litres of water. Vial 1 of ^{111}In, vial 4 of ^{131}I and the ^{134}Cs source were each placed in a tight plastic bag and then placed together in another tight plastic bag and taped to the vertical aluminium rod at an estimated 350 mm from the lid. Geometries for these measurements were created from the "Complex Cylinder" template (see Figure B1 in Appendix B). In the modelled geometry the spherical source had relative concentration 1.0 and was modelled to be 30 mm in diameter, placed at 350 mm height with 0 mm offset from the centre of the barrel and made of water with density 1.0 g/cm³. Surrounding the point source was a cylindrical layer of water, ρ=1.0 g/cm³, with height 680 mm. Four different geometries were created representing the four different sections in Figure 7. Measurements of these geometries were then performed at the four different sections by rotating the barrel 90° between measurements followed by a measurement when the barrel was rotating using a geometry identical to ones previously used. The sources were then removed and attached on the inside of the barrel at an estimated 350 mm height from the bottom. Geometries for these measurements were created from the "Complex Cylinder" (see Figure B2 in Appendix B). In the geometries the spherical source had relative concentration 1.0 and was modelled to be 30 mm in diameter and placed at 350 mm height with 220 mm offset from the centre of the barrel and at 0°, 90°, 180° and 270°

angular offset from the reference plane. The angular offset represents the different sections where 0°, 90°, 180° and 270° offset represents section 1, 2, 3 and 4 in accordance with Figure 8. Measurements of these geometries were then performed at the four different sections by rotating the barrel 90° after each measurement.

In order to determine if longer measurement time would affect the resulting activities, a measurement was performed during 1200 seconds at "R0-A" with the point source at the radial centre of the rotating barrel.

For the barrel with homogenous activity distribution vial 2 of ^{111}In and vial 3 of ^{131}I were mixed with 112 litres of water by diluting the liquid in the vials with the water followed by pouring the diluted nuclide mixture into the barrel and then stirring the contents with a plastic rod. 93 % of the radioactivity for ^{111}In was added to barrel as stated in Table 5, the missing 7 % was attached to the vial and estimated with a dose rate instrument. Two water samples were taken with 200 ml beakers as an independent measurement of the activity in the barrel of the assumed homogenised content. The geometries in ISOCS™ were made from the "Simple Cylinder" template (see Figure B1 in Appendix B) with one cylindrical layer of height 700 mm consisting of water, ρ=1.0 g/cm³, with relative concentration 1.0. Four different geometries were created representing the four different sections as before with the same measurement scheme.

The previous measurement scheme was performed at both "HA" and "R0-A"with no practical difference other than the pre-existing differences between the two sites, and that no measurement of the sources free in air was performed at "R0-A" and no long measurement was performed at "HA".

In addition to all measurements described above, the NaI(Tl) detector described in *4.2.1.3* was used to obtain additional information about the geometry.

4.4.2 Measurement on heterogeneous activity distributions using point sources

Setup 2 was performed on one barrel with heterogeneous activity distribution. For this setup the radionuclides used were ^{57}Co, ^{60}Co, ^{133}Ba and ^{137}Cs (see Table 4). These measurements were performed during one day and the reference time for the point sources activities was set to 12:00 that day, 12th of March 2015. The activities are presented in Table 6.

Table 6. The activities of the point sources used for the second set of measurements with reference time 12:00 the day of measurement, March 12 2015. The uncertainty for the activities is the total uncertainty at the 99 % confidence level given by the manufacturer Eckert & Ziegler Isotope Products, Inc.

Isotope	**Activity** [MBq]
^{57}Co	0.437 ± 3%
^{60}Co	1.610 ± 3%
^{133}Ba	2.455 ± 3%
^{137}Cs	3.355 ± 3%

All measurements described below were performed at the "R0-A" facility.

Before the sources were applied in the barrel a measurement was performed on all sources free in air in order to determine how well ISOCS™ could estimate the activity in the simplest reference geometry. The sources were placed in a plastic bag at the centre of the rotating table

on a wood balk on top of a stool at a distance of 148 cm from the detector. The point source was modelled from the "Sphere" template (see Figure 15 or Figure B3 in Appendix B) to be made of aluminium, ρ=2.7 g/cm³, with outside diameter 15 mm and shell thickness 0.01 mm made of polyethylene, ρ=0.92 g/cm³. The sphere was modelled at a distance of 148 cm from the detector and the table did not rotate.

The barrel was filled with 116 litres of water. The sources were placed together in a tight plastic bag and tied with a fishing line to sinkers a few centimetres beneath the vertical rod at a distance of 535 mm from the lid to the centre of the source. Geometries for these measurements were created from the template "Complex Cylinder" (see Figure B2 in Appendix B). In the geometry the spherical source was modelled to have a relative concentration of 1.0, having a diameter of 15 mm and being located at 165 mm height from the bottom of the barrel and with 0 mm offset from the centre of the barrel and made of aluminium with density 2.7 g/cm³. In the model, surrounding the source was a cylindrical layer of water with density 1.0 g/cm³ and height 650 mm. Four identical geometries were created representing the four different sections of the barrel in accordance with Figure 7 and the same measurement scheme as in section 4.4.1 for the corresponding measurement followed.

The source and sinkers were then removed and tied a few centimetres below the horizontal rod at peripheral radial distance at a distance of 510 mm from the lid to the centre of the source, with the source facing the detector. Geometries for these measurements were created from the "Complex Cylinder" template (see Figure B2 in Appendix B). In the geometries the spherical source had a relative concentration 1.0 and was modelled to be 15 mm in diameter, placed 190 mm from the bottom of the barrel with 225 mm offset from the centre of the barrel and at 0°, 90°, 180° and 270° angular offset from the reference plane representing section 1, 2, 3 and 4 in Figure 8. In the modelled geometries surrounding the source was a cylindrical 650 mm high layer of water with density 1.0 g/cm³. The same measurement scheme as in section 4.4.1 for the corresponding measurement followed.

In order to observe any potential difference in activity assessment for radionuclides with different energies the ^{57}Co source alone was measured. The source was put in a plastic bag and placed at peripheral radial position at a distance of 500 mm from the lid to the centre of the source. The measurement scheme was the same as previous measurements of the same type with the difference that the source was modelled to be 10 mm in diameter and positioned at 200 mm height from the bottom. The source was then placed in the radial centre of the barrel at a distance of 540 mm from the lid to the centre of the source. Two measurements were performed with this geometry; one with the barrel being stationary and one with rotating barrel. For these two measurements the modelled geometries were identical with the source at 160 mm height from the bottom.

The same scheme was then repeated with the ^{133}Ba source, with the source placed and modelled 150 mm from the bottom when placed in the radial centre of the barrel and at 200 mm when placed in the peripheral radial position. This source was also modelled to be 10 mm in diameter.

Lastly all sources were placed in a plastic bag and tied to the lid at a height of 500 mm from the bottom and measured once while stationary and once while rotating in order to observe any eventual difference from the sources vertical position. The modelled geometry was once again with the source diameter 15 mm.

In addition to all measurements described above, the NaI(Tl) detector described in *4.2.1.3* was used placed at height 80 cm from the centre of the detector to the floor to obtain additional information about the geometry.

4.4.3 Relative measurements comparing different matrices using an ^{18}F liquid source

These measurements were focused on assessing a relative difference between different geometries in order to obtain a factor between homogeneous activity distribution and a point source located in the radial centre. These measurements were performed on one barrel, in which two plastic bags were applied on the inside to avoid any radionuclide attachment to the inside of the barrel. The radionuclide used was ^{18}F (see Table 4) and due to the short half-life of this radionuclide a reference time was applied for compensation of the activity during measurement. The activity correction was made by the Genie™ software and measurements described below were performed at "R0-A" and a picture of the measurement setup is illustrated in Figure 16.

Figure 16. A picture of the measurement setup at "R0-A" for the third setup.

The barrel was filled with 100 litres of water and the cylindrical glass vial was placed in a plastic bag tied with fishing line to a weight. The bag with the vial was tied at height 345 mm from the bottom with fishing line to the lid and placed without offset from the radial centre. The geometry for this measurement was created from the template "Complex Cylinder" (see Figure B2 in Appendix B). In the geometry a spherical source was modelled with a relative concentration of 1.0, having a diameter of 10 mm and located at 345 mm height from the bottom of the barrel and with 0 mm offset from the centre of the barrel and made of water with density 1.0 g/cm³. In the model surrounding the source was a cylindrical layer of water with density 1.0 g/cm³ and height 580 mm. A measurement of this geometry was performed while the barrel was rotating.

The source was then moved to a peripheral radial distance with the same height from the bottom as in the previous measurement with the source facing the detector. The geometry for this measurement was created from the "Complex Cylinder" (see Figure B2 in Appendix B). The modelled geometry was the same as above but with 225 mm offset from the centre of the barrel and the measurement of this geometry was performed with rotating barrel.

Then the vial was mixed with the water by diluting the liquid in the vial with the water and emptying it in the barrel followed by stirring the contents with a plastic rod. Two water samples with 200 ml beakers were then taken as an independent measurement of the activity of the assumed homogenised content. For the measurement of this homogeneous activity distribution a geometry was created from the "Simple Cylinder" template (see Figure B1 in Appendix B) with one cylindrical layer of height 580 mm consisting of water with density 1.0 g/cm³ and with relative concentration 1.0. A measurement of this geometry was performed while the barrel was rotating.

In addition at all measurements described above, the NaI(Tl) detector described in *4.2.1.3* was used. The detector was placed at height 82 cm from the centre of the detector to the floor and the measurement with this detector was performed with a live time of 5 seconds that looped continuously thus giving an assessment of the contents variation.

4.4.4 Measurements to estimate the reproducibility

To estimate the reproducibility for the sorts of measurements performed in this work two setups were used with set parameters and then repeating the same measurements a number of times dismantling the setup between each measurement. The first setup was with three point sources, one ^{60}Co and two ^{137}Cs, taped to the wall of the barrel at height 35 cm facing the detector. The distance from the floor to the top of the detector was decided to be 70 cm and the distance from the detector end cap to the barrel was decided to be 60 cm. This setup was measured 10 times.

The second setup was with the same point sources placed at the same height but placed 90° in relation to the detector. The height was changed to 75 cm and the distance remained unchanged. This setup was measured 8 times.

4.5 Analysis

All water samples were independently analysed by the Radiometrics department at Studsvik Nuclear AB by means of laboratory spectrometry with HPGe detectors[4].

The spectra from ISOCS™ were analysed by an analysis sequence in the Genie™ 2000 software system. For the Genie™ 2000 software system used, see Appendix C. For more information on the analysis steps and their algorithms, they are described in detail in the *Genie™ 2000 Customization Tools Manual*[45].The sequence consist of six steps and they were as follows:

i. Peak locate algorithm "Generalized Second Difference Method".
ii. Peak area algorithm "Sum/Non-Linear Least Squares Fit Peak Area".
iii. Area correction algorithm "Standard Background Subtract".
iv. Efficiency correction algorithm "Standard Efficiency Correction".
v. Nuclide identification algorithm "Nuclide Identification with Interference Correction".
vi. Reporting the previous analysis steps.

For analysis of the results from the NaI(Tl) detector MAESTRO-32 was used to extract the total number of counts from the collected spectra for the first two sets of measurement whereas a script in Python 3.4 was used to extract the total number of counts for the third setup. MAESTRO-32 was also used to extract the total number of counts for the measurements to estimate the reproducibility.

[4] The Radiometrics department at Studsvik Nucelar AB is an accredited laboratory

5 Results and discussion

In the figures below where denoted ”Average” is the average of section 1, section 2, section 3 and section 4. In the cases where not all sections are quantified the average value refers to the average of the sections that are quantified. The activity calculated by ISOCS™ is a weighted mean activity with all photon energies for the respective radionuclide presented in Table 4. All error bars and uncertainties are based upon the estimated error in placing the barrel at the rotational centre, taken from the case with homogeneous activity distribution in Figure 28 and assuming this to be applicable to all measurements except the “free in air” measurements. Also the estimated uncertainty in placement of the sources were added by calculating the attenuation for the most significant highest energy for the respective radionuclide for the heterogeneous activity distributions, where the uncertainty was estimated to be 2 cm for ^{111}In, ^{131}I and ^{134}Cs and 1 cm for the other radionuclides. In addition, the error bars also includes uncertainties in counting statistics from the resulting spectra and are within 2 standard deviations.

5.1 Measurements on two different matrices using ^{111}In, ^{131}I and ^{134}Cs

5.1.1 HA

Figure 17 to Figure 19 and Table 7 below illustrates the deviation from the reference activity estimated by ISOCS™ at the “HA” facility for the first setup and Table 8 to Table 10 shows the total number of counts for the NaI(Tl) detector for the corresponding measurement.

5.1.1.1 Sources free in air

Table 7. The table shows how much ISOCS™ deviate from the reference activity (vial 2 with ^{111}In, vial 3 with ^{131}I and the point source of ^{134}Cs in Table 5) when the sources are placed free in air at “HA”.

Nuclide	**Deviation from reference activity** [%]
^{111}In	16.77 ± 0.40
^{131}I	- 1.85 ± 0.55
^{134}Cs	- 4.09 ± 1.05

With the sources placed free in air the deviation from the reference value seems to depend upon the energies of the radionuclide. With the lower energies of ^{111}In, the activity is overestimated whereas the higher energies of ^{131}I lead to an underestimation and the energies from ^{134}Cs lead to the largest underestimation. However, the steel table upon which the sources were placed contributed to an error in this setup. Since this measurement was modelled without the table it is likely that the table has attenuated some of the radiation emitted from the sources. This would have an effect on the number of photons incident on and registered by the detector, as the sources was placed an estimated 2 cm or so from the edge of the table. It is therefore assumed that a measurement that is more truly free in air would overestimate the activity of ^{111}In more than Table 7 whereas there would be no underestimation of the activity for ^{131}I and ^{134}Cs.

5.1.1.2 Sources placed at radial centre

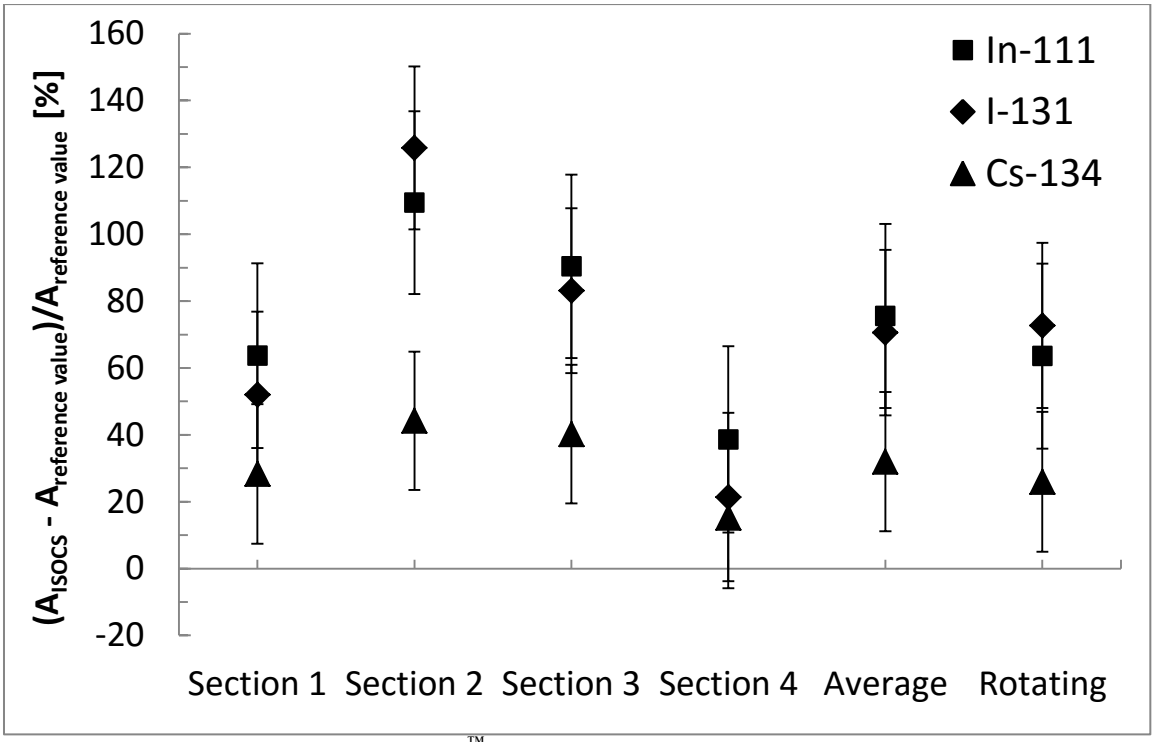

Figure 17. A graph over how much ISOCS™ activity estimation deviate from the reference activity (vial 1 with ^{111}In, vial 4 with ^{131}I and the point source of ^{134}Cs in Table 5) for different measurement geometries where the sources are placed in the radial centre of the barrel at "HA".

Table 8. The total number of counts for the Ø 76.2 mm x 76.2 mm NaI(Tl) detector for different measurement geometries where vial 1 with ^{111}In, vial 4 with ^{131}I and the ^{134}Cs point source from Table 5 are placed in the radial centre of the barrel at "HA".

Geometry	**Total number of counts**
Section 1	$4.07 \cdot 10^6$
Section 2	$5.59 \cdot 10^6$
Section 3	$5.57 \cdot 10^6$
Section 4	$3.93 \cdot 10^6$
Average	$4.79 \cdot 10^6$
Rotating	$4.78 \cdot 10^6$

As Figure 17 indicates, there is a clear deviation from the reference value of the sources when they are placed in the radial centre of the barrel. The general observation is that section 2 yields the highest deviation, section 3 yields the second highest deviation, section 1 yields the second lowest deviation and section 4 yields the lowest deviation. This is true for all three nuclides. There is a substantial variation in deviation with the different sections but it is evident that ^{134}Cs varies less than the others. To conclude, there seems to exist an energy dependence here as well. The similarity between an average of all sections and when the barrel was rotating indicates that the sources geometrical (radial) placement was not the same during the different sections, which was the underlying assumption with the sources placed in the radial centre. In practice this displacement is explained by the aluminium rod in the lid to

which the sources were attached. Presumably the rod attenuated some of the radiation but when studying Figure 17 this effect seems to be of less importance.

Table 8 supports the discussion concerning the displacement of the sources as the same pattern is visible here, although the results show a lower relative difference between the sections. This is because the table do not show the nuclide specific counts rather than the total number of counts and thus says nothing about the variations for the individual radionuclides.

5.1.1.3 Sources placed in the radial periphery

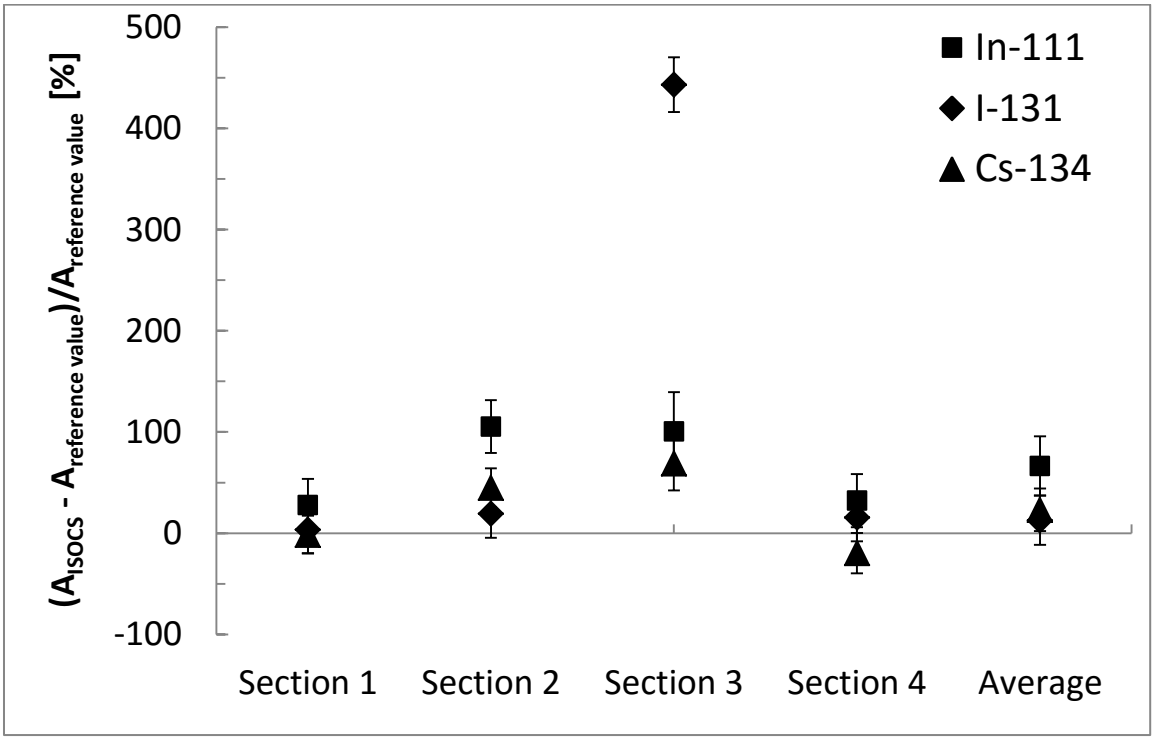

Figure 18. A graph over how much ISOCS™ activity estimation deviate from the reference activity (vial 1 with ^{111}In, vial 4 with ^{131}I and the point source of ^{134}Cs in Table 5) for different measurement geometries where the sources are placed in the radial periphery of the barrel at "HA".

Table 9. The total number of counts for the Ø 76.2 mm x 76.2 mm NaI(Tl) detector for different measurement geometries where vial 1 with ^{111}In, vial 4 with ^{131}I and the ^{134}Cs point source from Table 5are placed in the radial periphery of the barrel at "HA". The x indicates no value (due to a mistake made by the author).

Geometry	Total number of counts
Section 1	$23.4 \cdot 10^6$
Section 2	x
Section 3	$1.18 \cdot 10^6$
Section 4	$3.50 \cdot 10^6$
Average	$9.36 \cdot 10^6$
Rotating	$7.77 \cdot 10^6$

With the sources placed in the radial periphery there exists great variations between the different sections. In general there is an overestimation of activity but some individual results show very good agreement as two values (^{131}I and ^{134}Cs) in section 1 agrees with the reference value within 5 %. The results indicate that ISOCS™ presents an accurate estimation

when there is minimum attenuating material between the source and the detector. This is a reasonable result as this was the simplest geometry to model (thus to achieve a correspondence with the reference activity content). The outlier result with ^{131}I in section 3 cannot be explained. The reader should note that the average for ^{131}I is calculated without this extreme value. Also note that section 2 and section 4 should, in theory, give the same value as these are the same geometry (although mirrored, see Figure 7). The difference is explained by the aluminium rod which caused a displacement of the sources between these measurements, favouring and disfavouring the different nuclides at different sections thus introducing an error in the geometry compared to the model.

Table 9 is not complete and unfortunately it is one of the theoretically identical geometries that are missing. However, it is possible to deduce that section 1 yields the most counts and section 3 the least, as expected.

5.1.1.4 Homogeneous activity distribution

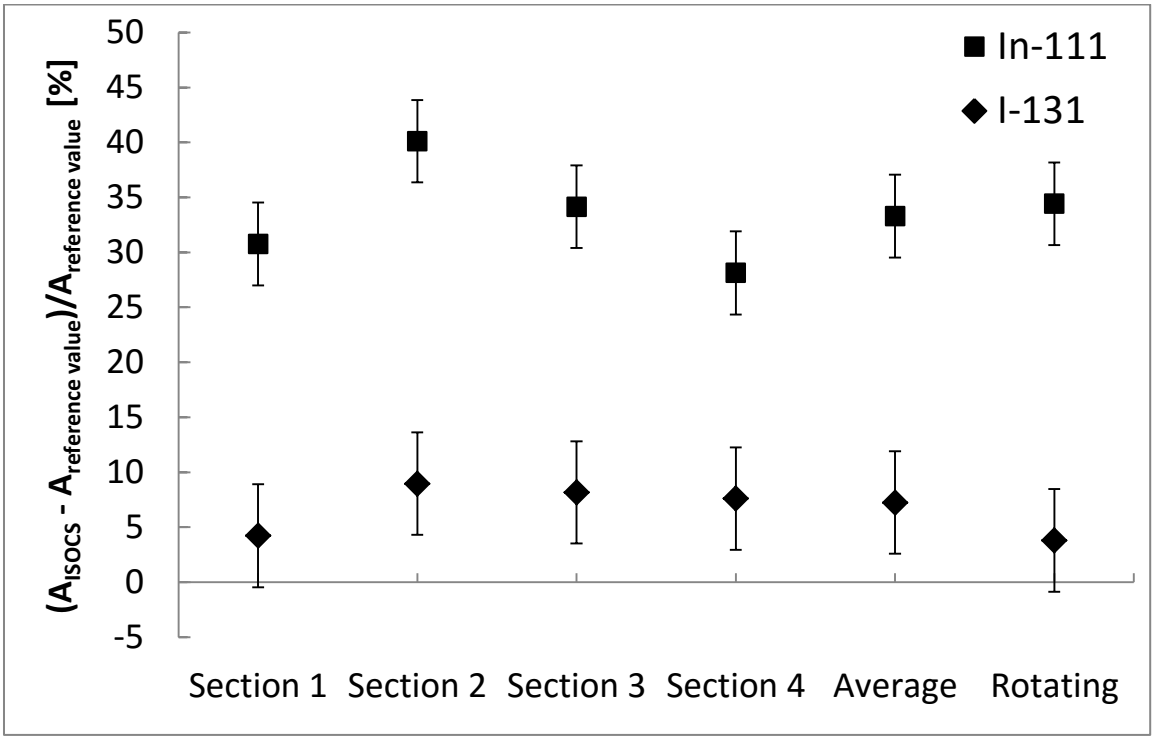

Figure 19. A graph over how much ISOCS™ activity estimation deviate from the reference activity (vial 2 with ^{111}In and vial 3 with ^{131}I in Table 5) for different measurement geometries with homogeneous activity distribution at "HA".

Table 10. The total number of counts for the Ø 76.2 mm x 76.2 mm NaI(Tl) detector for different measurement geometries with homogeneous activity distribution of vial 2 with ^{111}In and vial 3 with ^{131}I in Table 5 at "HA".

Geometry	Total number of counts
Section 1	$4.66 \cdot 10^6$
Section 2	$5.03 \cdot 10^6$
Section 3	$4.87 \cdot 10^6$
Section 4	$4.58 \cdot 10^6$
Average	$4.79 \cdot 10^6$
Rotating	$4.78 \cdot 10^6$

Figure 19 shows results that are a great improvement compared to earlier, both in relative and in absolute numbers. Figure 19 indicates that the activity content is indeed homogeneous and the activity content is well estimated by ISOCS™, at least when it comes to ^{131}I. Unfortunately there is still some variation for ^{111}In and comparing the results to ^{131}I the variation cannot be explained by displacement of the barrel, i.e. that the barrel was not placed at the rotational centre. It is therefore most likely that some of solution containing ^{111}In has formed "hot spots" with activity. It was later confirmed that this solution lacked a sufficient chemical carrier that would have hampered the solution to attach to plastic.

Table 10 supports the assumption that the content in homogeneous. Although there is some variation here as well it needs to be seen in comparison to Table 8 and Table 9. From this comparison it is strongly indicated that the variation in Table 10 is too small to be able to claim the content as anything else than homogeneous.

5.1.2 R0-A

Figure 20 to Figure 22 below illustrates the deviation from the reference activity estimated by ISOCS™ at the "R0-A" facility for the first setup and Table 11 to Table 13 shows the total number of counts for the NaI(Tl) detector for the corresponding measurement.

5.1.2.1 Sources placed at radial centre

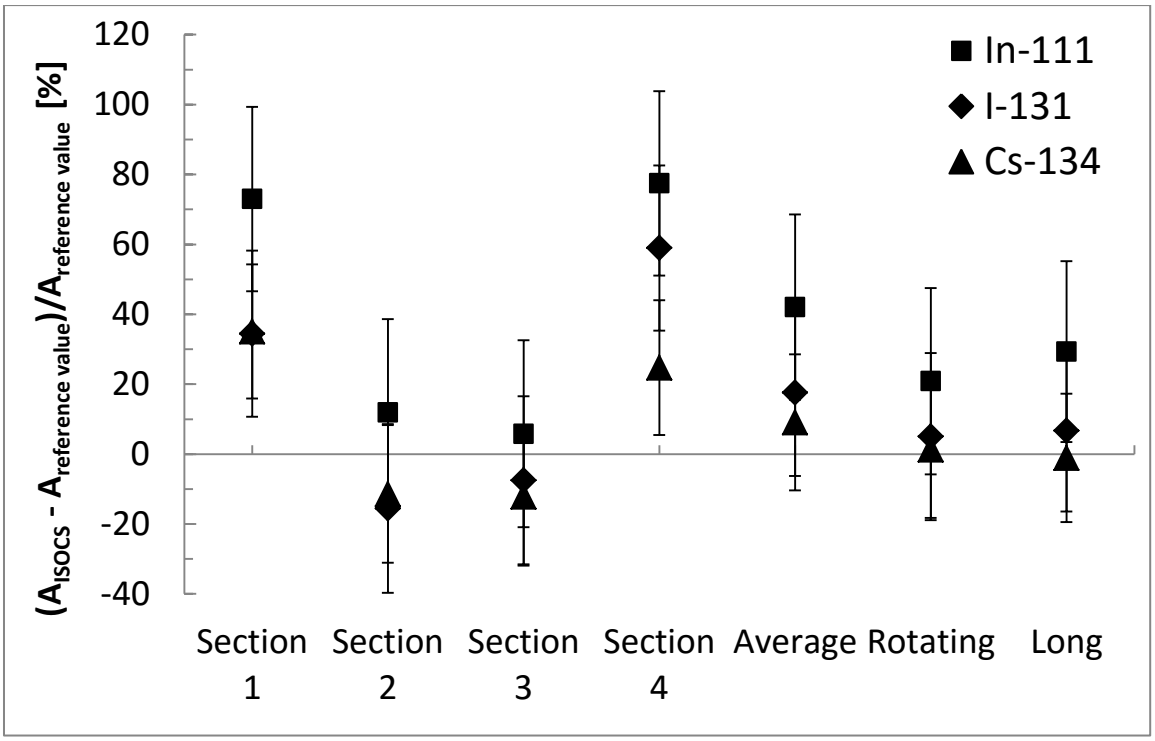

Figure 20. A graph over how much ISOCS™ activity estimation deviate from the reference activity (vial 1 with ^{111}In, vial 4 with ^{131}I and the point source of ^{134}Cs in Table 5) for different measurement geometries where the sources are placed in the radial centre of the barrel at "R0-A".

Table 11. The total number of counts for the Ø 76.2 mm x 76.2 mm NaI(Tl) detector for different measurement geometries where vial 1 with ^{111}In, vial 4 with ^{131}I and the ^{134}Cs point source from Table 5are placed in the radial centre of the barrel at "R0-A".

Geometry	Total number of counts
Section 1	$2.54 \cdot 10^6$
Section 2	$1.76 \cdot 10^6$
Section 3	$1.56 \cdot 10^6$
Section 4	$2.31 \cdot 10^6$
Average	$2.04 \cdot 10^6$
Rotating	$2.02 \cdot 10^6$

In Figure 20 there is a predominant variation between the different sections, as observed at "HA". In this case the general pattern is that in section 1 and 4 differ from the reference value is by a somewhat equal amount. This is also true for section 2 and 3 but with an underestimation of activity for ^{131}I and ^{134}Cs. Also the variations are greatest for ^{111}In and the least for ^{134}Cs. The probable explanation for this is once again assumed to be displacement of the sources due to the aluminium rod. Because of the smaller distance between the barrel and the detector it is possible that the barrel was not properly centred on the rotation table which could explain part of the variations. There is a better correspondence for the measurement when the barrel was rotating than for the average value of the sections. The reason for this result has not yet been discovered. Neither can it be explained that the deviation is slightly bigger when the measurement time increases fourfold. Logically the correspondence would be better with more time as it yields better counting statistics.

Table 11 shows the same general pattern as Figure 20 where section 1 and 4 are similar in their total number of counts, as is section 2 and 3. It therefore seems that the displacement is such that section 2 and 3 are disadvantaged whereas section 1 and 4 are not. Here though, the average and rotating value show better correspondence but once again it is worth pointing out that this is the total number of counts and can thus not be applied to the individual radionuclides, which would be needed in order to connect this to the discussion for Figure 20.

5.1.2.2 Sources placed in the radial periphery

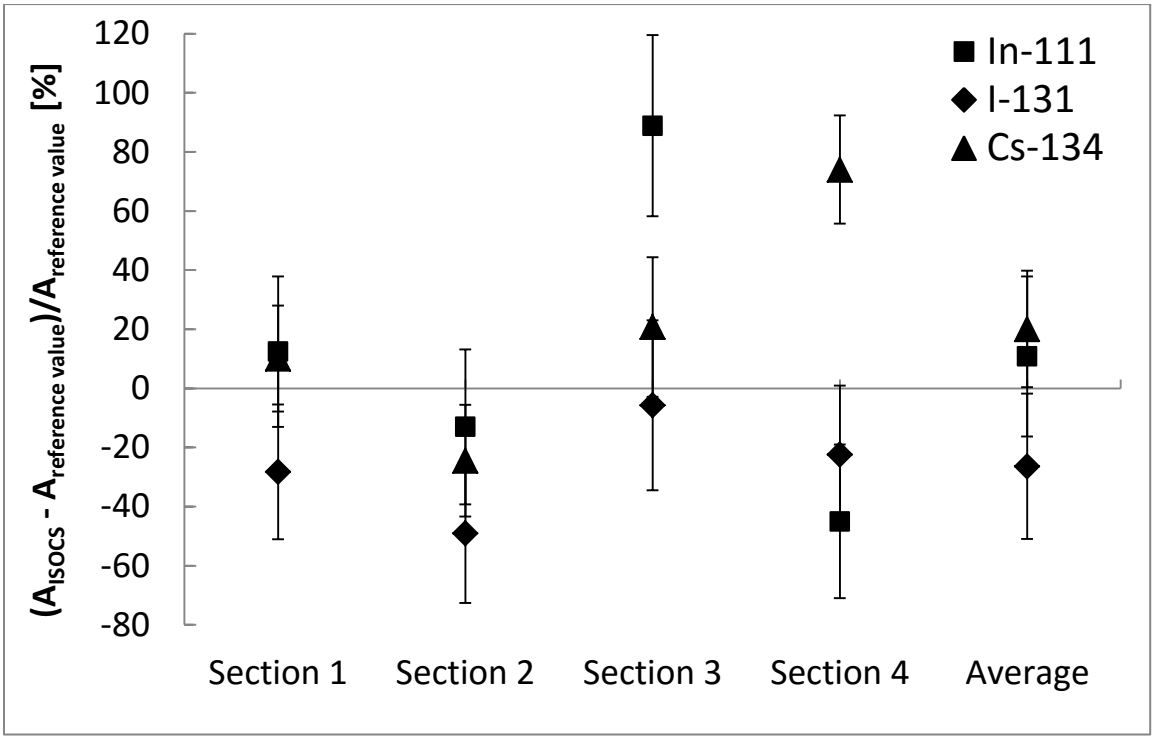

Figure 21. A graph over how much ISOCS™ activity estimation deviate from the reference activity (vial 1 with ^{111}In, vial 4 with ^{131}I and the point source of ^{134}Cs in Table 5) for different measurement geometries where the sources are placed in the radial periphery of the barrel at "R0-A".

Table 12. The total number of counts for the Ø 76.2 mm x 76.2 mm NaI(Tl) detector for different measurement geometries where vial 1 with ^{111}In, vial 4 with ^{131}I and the ^{134}Cs point source from Table 5are placed in the radial periphery of the barrel at "R0-A".

Geometry	**Total number of counts**
Section 1	$7.81 \cdot 10^6$
Section 2	$2.68 \cdot 10^6$
Section 3	$0.41 \cdot 10^6$
Section 4	$1.32 \cdot 10^6$
Average	$3.05 \cdot 10^6$

The individual radionuclide variations are too great in order to claim any general pattern from Figure 21. For ^{111}In there is good correspondence for section 1 and 2 but a 100 % overestimation for section 3 and then a 50 % underestimation for section 4. For ^{131}I the activity is underestimated for all sections but most for section 2, close to unity for section 3 and around 25 % for both section 1 and 4. Then for ^{134}Cs the variations are uncharacteristically large with around 75 % overestimation for section 4, 25 % underestimation for section 2 and the same percentage but positive in section 3 and lastly good agreement in section 1. These individual variations can only be explained in that the sources must have been placed in such a way that different radionuclides have been favoured and disfavoured in different sections. This is supported by sections 2 and 4 which in theory should be the same but this is hardly the case in Figure 21, although displacement of the barrel on the rotational table should not be ignored as a source of error. If ^{134}Cs was placed closest to the detector when measuring section 4 in conjunction with the potential

displacement of the barrel, this could explain less attenuating material than modelled thus leading to an overestimation of activity.

From Table 12 it is clear that section 2 and 4 are not equivalent as they differ by a factor 2 in total number of counts. Otherwise the pattern supports the theory with substantially more counts in section 1 than section 3 and a "middle ground" for section 2 and 4.

5.1.2.3 Homogeneous activity distribution

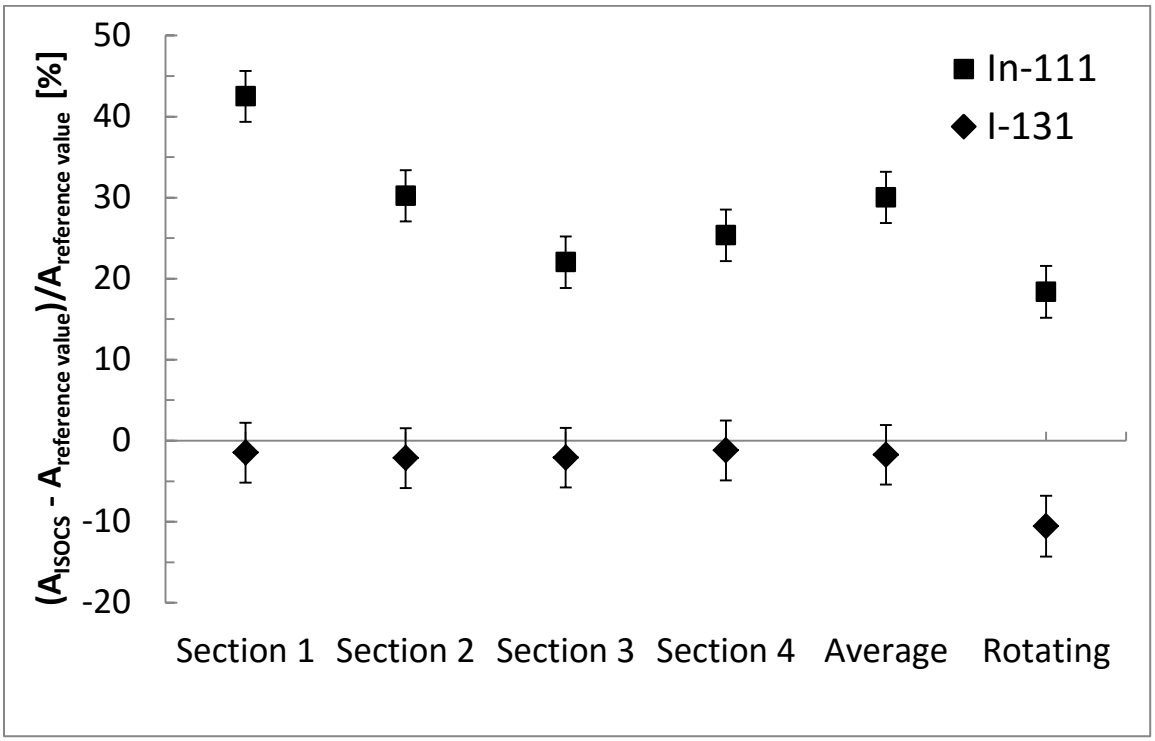

Figure 22. A graph over how much ISOCS™ activity estimation deviate from the reference activity (vial 2 with ^{111}In and vial 3 with ^{131}I in Table 5) for different measurement geometries with homogeneous activity distribution at "R0-A".

Table 13. The total number of counts for the Ø 76.2 mm x 76.2 mm NaI(Tl) detector for different measurement geometries with homogeneous activity distribution of vial 2 with ^{111}In and vial 3 with ^{131}I in Table 5 at "R0-A".

Geometry	**Total number of counts**
Section 1	$2.06 \cdot 10^6$
Section 2	$1.99 \cdot 10^6$
Section 3	$1.85 \cdot 10^6$
Section 4	$1.88 \cdot 10^6$
Average	$1.94 \cdot 10^6$
Rotating	$1.93 \cdot 10^6$

Figure 22 indicates that the ^{111}In is not homogeneously distributed in analogy with the discussion for Figure 19. It is clear that the radioactivity has formed some "hot spots" in the plastic which causes this variation. For ^{131}I the agreement is very good for all sections. And because there is practically no variation between the sections, this barrel was not displaced on the rotating table which could otherwise have explained some of the variation for ^{111}In. It is confusing that the value decreases when the barrel is rotating. An explanation for this cannot

be presented but a theory is that the E-field from the electric motor that drives the rotating table has interfered with the detector and/or the pulse electronics. This has not yet been confirmed.

Table 13 also clearly indicates homogeneity as there is exceptionally little variation between the sections.

5.1.3 Water samples

Table 14 below shows the analysis results from the water samples taken with two 200 ml beakers when vial 2 with ^{111}In and vial 3 with ^{131}I had been mixed with water.

Table 14. The analysis results after mixing ^{111}In and ^{131}I with water (vial 2 and vial 3 in Table 5). These results were obtained from the Radiometrics department at Studsvik Nuclear AB.

Beaker #	**Detector #**	**Nuclide**	**Activity Concentration** [Bq/ml]
1	1	^{111}In	99.5
		^{131}I	70.6
	2	^{111}In	97.8
		^{131}I	71.3
2	1	^{111}In	104
		^{131}I	72.0
	2	^{111}In	102
		^{131}I	71.5

All values in Table 14 are to be considered having a type B uncertainty of 7 %, based upon calibration of the detectors used and the estimated volume of the samples.

With the assumption that the barrel contained 112 litres of water, the average total activity of ^{111}In was 11.29 MBq and for ^{131}I the average total activity was 7.99 MBq.

The individual variations between the beakers and the detectors imply that the radionuclide content was homogeneously distributed in the water. In compliance with earlier discussion there is a larger variation for ^{111}In here as well, although not by much and within the uncertainty. The values 11.29 MBq and 7.99 MBq should be compared to 93 % of 10.5 MBq and 8.45 MBq in Table 5. With the 7 % type B uncertainty from the beaker measurement and the uncertainty in determining the volume 112 litres these values can be considered to be in good agreement and therefore an independent verification that the content was homogenously distributed in the water.

5.1.4 Final remarks

From the first setup it is clear that there is room for improvement. It is desired to first and foremost try to reduce the variations from section to section and it is concluded that the aluminium rods are the biggest source of perturbation for the Canberra ISOCS™ system in estimating the reference activity. So reducing the impact from these would be a logical next step. The easiest way to do this is presumed to be to place the sources below the rods. So drilling a hole at the end of each rod would enable hanging future sources in a thread below the rods. This was the primary thought leading to the second setup. To be more thorough and

measure instead of estimating the size of the source(s) and offsets is also an important lesson learned from this setup and will hopefully reduce the deviation in conjunction with diminishing the impact of the aluminium rods. Another thought was that it would be easier to have sources that did not decay during the experiments and that had a wider array of energies leading to the use of traceable point sources. It is also a bit unfortunate to use nuclides in solutions to create matrices with homogeneous activity distribution and not investigate whether they stuck to the plastic or not. A notation to the homogeneous activity distribution is that for Figure 19 and Figure 22 the reference values are from Table 5 when the value from the laboratory measurements could have been used as well. If this had been the case the deviation of activity for ^{111}In would have been around 21 % at the most.

5.2 Measurement on heterogeneous activity distributions using point sources

5.2.1 Sources free in air

Table 15 below shows the deviation from the reference activity for ISOCS™ for point sources placed free in air at "R0-A".

Table 15. The table shows how much ISOCS™ deviate from the reference activity when the point sources in Table 6 are placed free in air at "R0-A".

Nuclide	**Deviation from reference activity** [%]
^{57}Co	7.51 ± 1.45
^{60}Co	2.50 ± 1.49
^{133}Ba	14.22 ± 0.68
^{137}Cs	3.59 ± 1.20

With the sources free in air at "R0-A" Table 15 indicates that there is generally very good agreement with the sources reference activity and the activity estimated by ISOCS™. The poor agreement for ^{57}Co is presumed to be due to the substantial Compton contribution at its low energies. The high deviation for ^{133}Ba cannot be explained as the many energy lines from this radionuclide are weighted together assuring that the 356 keV line will have most impact in the activity estimation.

5.2.2 Sources placed at radial centre

Figure 23 and Table 16 below shows the deviation from the reference activity estimated by ISOCS™ and the total number of counts for the NaI(Tl) detector when the sources are placed at the radial centre of the barrel at "R0-A".

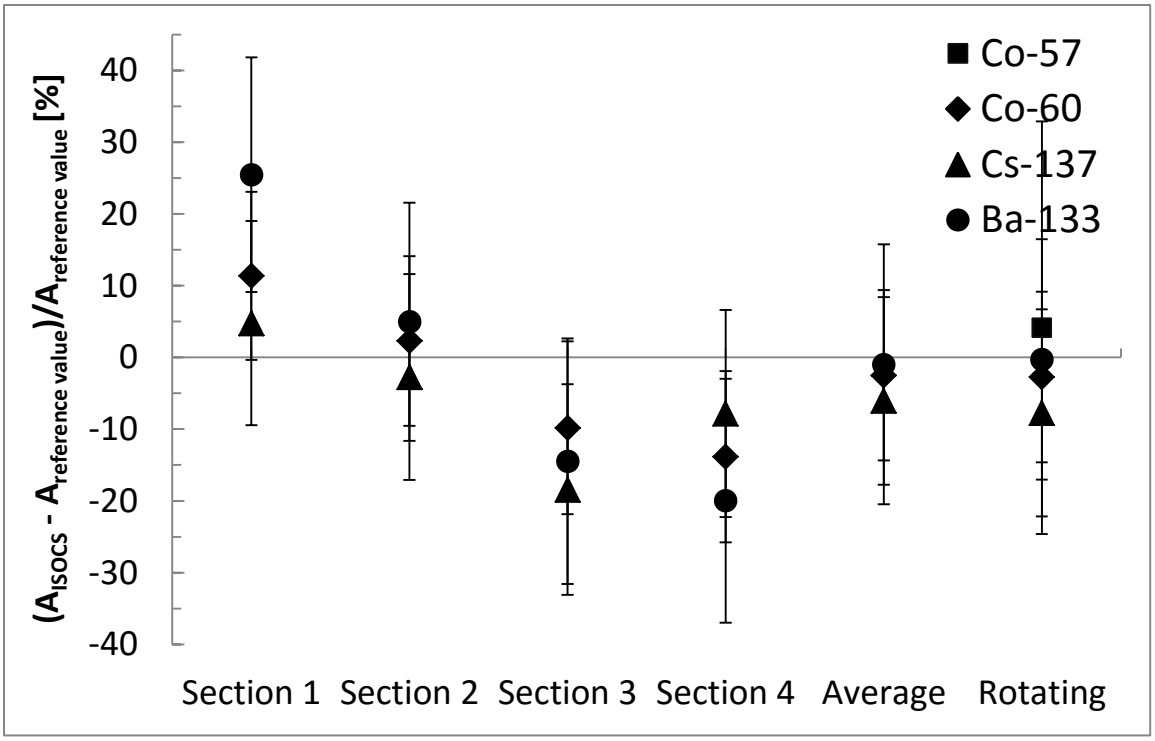

Figure 23. A graph over how much ISOCS™ activity estimation deviate from the reference activity for different measurement geometries where the point sources in Table 6 are placed in the radial centre of the barrel at "R0-A". The results for ^{57}Co are omitted from section 1, section 2 and section 3 because of low counting statistics and were not quantified for section 4.

Table 16. The total number of counts for the Ø 76.2 mm x 76.2 mm NaI(Tl) detector for different measurement geometries where the point sources in Table 6 are placed in the radial centre of the barrel at "R0-A".

Geometry	**Total number of counts**
Section 1	$5.55 \cdot 10^5$
Section 2	$5.38 \cdot 10^5$
Section 3	$4.84 \cdot 10^5$
Section 4	$4.97 \cdot 10^5$
Average	$5.19 \cdot 10^5$
Rotating	$5.20 \cdot 10^5$

When the sources are placed at the radial centre it is indicated from Figure 23 that all radionuclides apart from ^{57}Co follow the same pattern with most overestimation in section 1 followed by a decrease to section 2 and 3 and then a slight decrease to section 4. This is true apart from ^{137}Cs which increases between section 3 and 4. Although there are variations they are to be compared to the results from the first setup. Comparing the two, it is clear that the variations between the sections has decreased although this not an apples-to-apples comparison since other radiation sources are used here. Regarding ^{57}Co the point source has too low activity resulting in poor counting statistics so the source itself is poorly chosen because of this. Once again the explanation for the variation is displacement of the sources, which is strongly indicated by the average values which are in very good agreement with the values for when the barrel was rotating. A calculation was also performed to determine how much water was needed in order to attenuate the radiation as much as the difference between

sections 1 and 3 and the thickness of water needed was just over 2 cm which is a radial displacement that cannot be excluded (hence the error bars). Neither can a displacement of the barrel itself of a centimetre or two from the rotational centre be excluded.

The indication from Table 16 is that there are still variations but that they are much less than before. A comparison with Table 11 indicates that the greatest difference between two sections is around 15 % here compared to 63 % for the first setup. Table 16 also supports that the variations can be explained by the displacement of the sources or the barrel as the average and rotating value are near identical.

5.2.3 Sourced placed in the radial periphery

Figure 24 and Table 17 below shows the results presented by ISOCS™ and the total number of counts for the NaI(Tl) detector when the sources are placed in the radial periphery of the barrel at "R0-A".

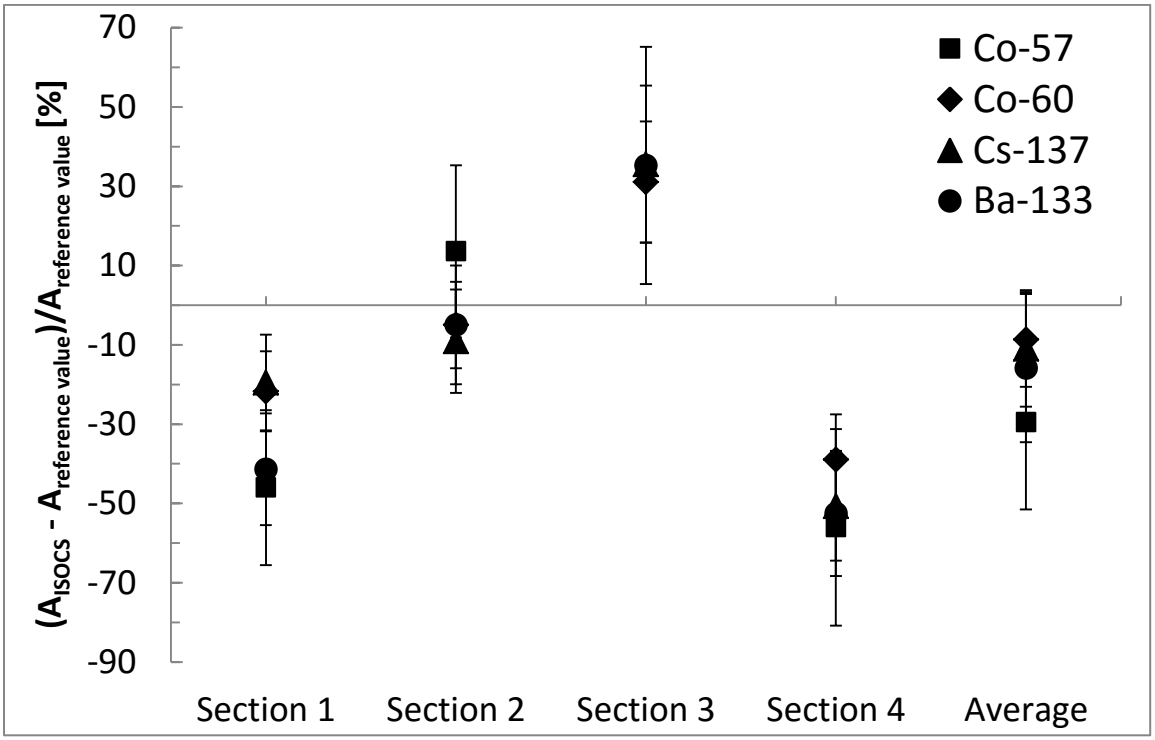

Figure 24. A graph over how much ISOCS™ activity estimation deviate from the reference activity for different measurement geometries where the point sources in Table 6 are placed in the radial periphery of the barrel at "R0-A".

Table 17. The total number of counts for the Ø 76.2 mm x 76.2 mm NaI(Tl) detector for different measurement geometries where the point sources in Table 6 are placed in the radial periphery of the barrel at "R0-A".

Geometry	Total number of counts
Section 1	$1.44 \cdot 10^6$
Section 2	$0.95 \cdot 10^6$
Section 3	$0.16 \cdot 10^6$
Section 4	$0.29 \cdot 10^6$
Average	$0.71 \cdot 10^6$

When the sources are placed in the radial periphery Figure 24 shows that once again the activity estimation varies greatly between the different sections. The general pattern is that from section 1 the activity estimation increases to section 2 and again to section 3 and then decreases to a minimum at section 4. That ^{57}Co is not included from section 3 is because of its low energies that will not in sufficient quantity penetrate roughly 45 cm of water. The difference between section 2 and 4 is very large and indicates that the placement of the sources was not precise enough or that the barrel was displaced significantly. But the last reason is not supported by the discussion for when the sources were in the radial centre as the barrel had the exact same placement for these measurements. That section 1 deviates as much as it does is a bit concerning and could also be an indication that the sources were not placed with adequate precision (in correspondence with the model).

From Table 17 the desired difference between sections 1 and 3 is observed. The value for section 4 is three times lower than for section 2 whereas it is closer to the value for section 3. So clearly a significant displacement occurred when the sources were positioned.

5.2.4 ^{57}Co and ^{133}Ba measurements

Figure 25 and Figure 26 illustrates the deviation from the reference activity estimated by ISOCS™ for measurements of different geometries with ^{57}Co and ^{133}Ba. Table 18 and Table 20 shows the total number of counts recorded with the NaI(Tl) for the measurements with ^{57}Co whereas Table 19 and Table 21 shows the same for the measurements with ^{133}Ba.

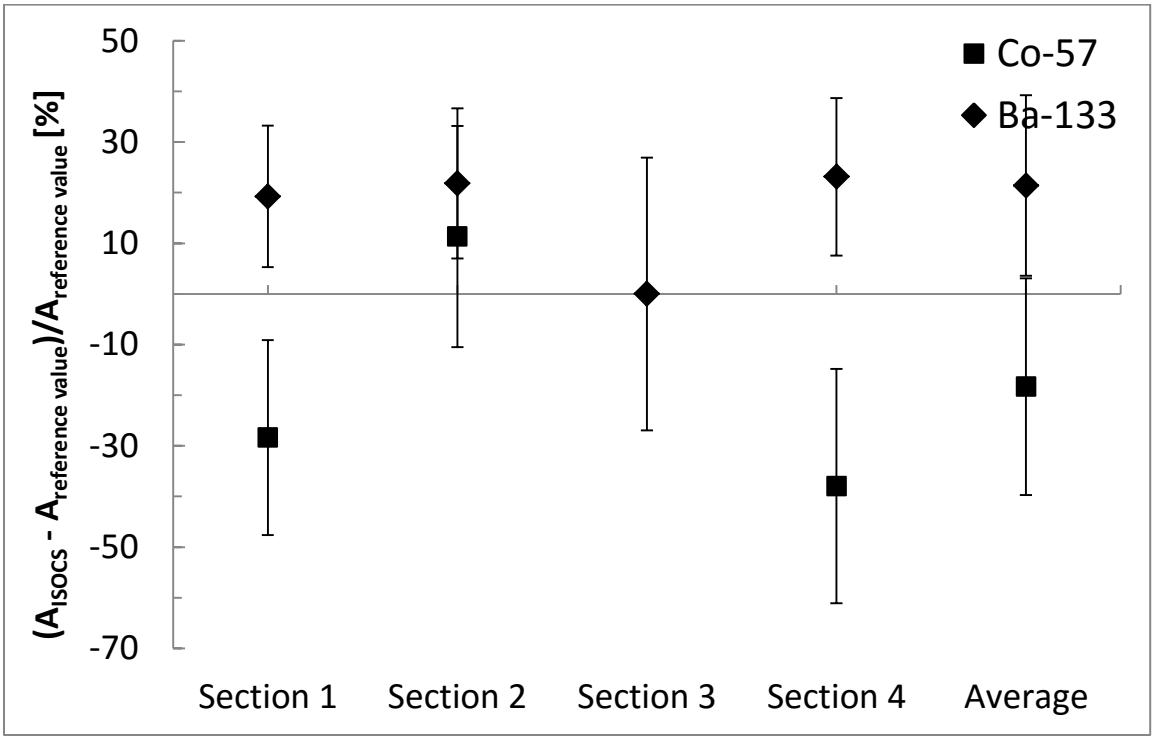

Figure 25. A graph over how much ISOCS™ activity estimation deviate from the reference activity for different measurement geometries and individual measurements with the ^{57}Co and the ^{133}Ba source from Table 6 placed in the radial periphery of the barrel at "R0-A".

Table 18. The total number of counts for the Ø 76.2 mm x 76.2 mm NaI(Tl) detector for different measurement geometries with the ^{57}Co source from Table 6 placed in the radial periphery of the barrel at "R0-A".

Geometry	**Total number of counts**
Section 1	$60.4 \cdot 10^3$
Section 2	$25.1 \cdot 10^3$
Section 3	$3.31 \cdot 10^3$
Section 4	$6.95 \cdot 10^3$
Average	$23.9 \cdot 10^3$

Table 19. The total number of counts for the Ø 76.2 mm x 76.2 mm NaI(Tl) detector for different measurement geometries with the ^{133}Ba source from Table 6 placed in the radial periphery of the barrel at "R0-A".

Geometry	**Total number of counts**
Section 1	$4.90 \cdot 10^5$
Section 2	$2.76 \cdot 10^5$
Section 3	$0.27 \cdot 10^5$
Section 4	$0.59 \cdot 10^5$
Average	$2.13 \cdot 10^5$

With individual sources Figure 25 shows a systematic behaviour in analogy with Figure 24 as the deviation is very similar between the figures for the radionuclides involved. Concluded, the multitude of sources present at earlier measurements has not affected the results for the individual radionuclides, although under assumption that the placement of the sources was identical.

The discussion for Table 18 and Table 19 are in analogy with the discussion concerning Table 17.

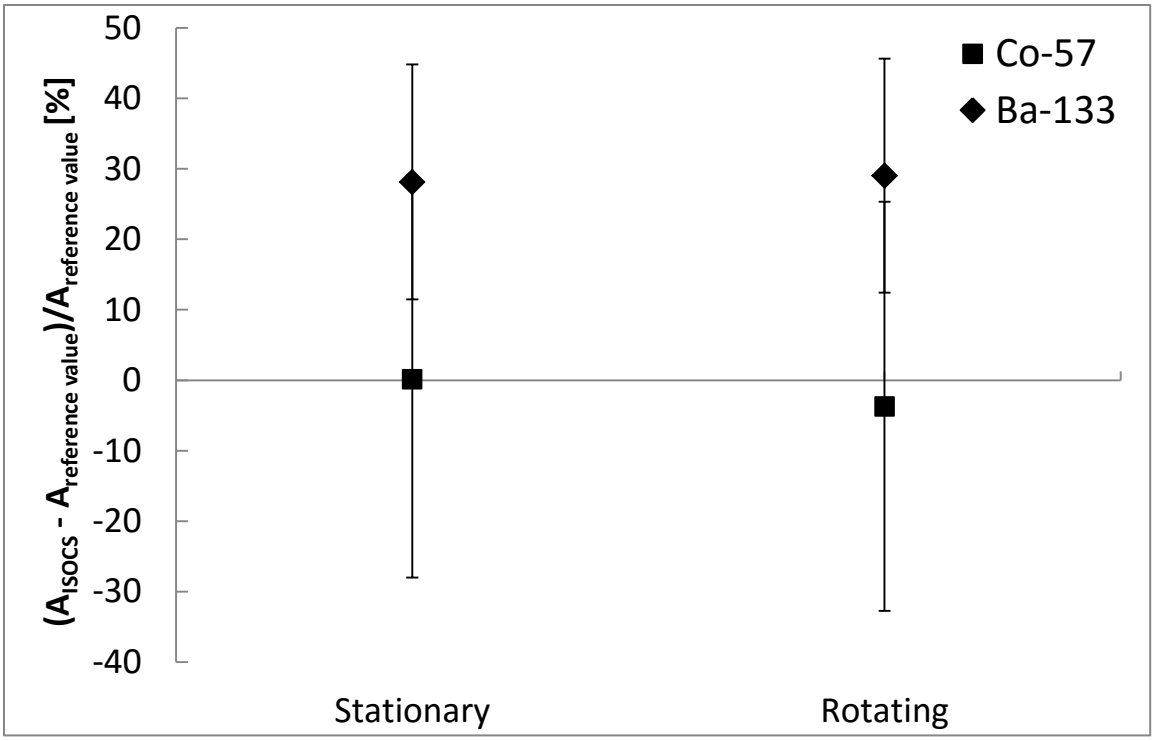

Figure 26. A graph over how much ISOCS™ activity estimation deviate from the reference activity for different measurement geometries and individual measurements with the ^{57}Co and the ^{133}Ba source from Table 6 placed in the radial centre of the barrel at "R0-A".

Table 20. The total number of counts for the Ø 76.2 mm x 76.2 mm NaI(Tl) detector for different measurement geometries with the ^{57}Co source from Table 6 placed in the radial centre of the barrel at "R0-A".

Geometry	**Total number of counts**
Stationary	$9.10 \cdot 10^3$
Rotating	$9.19 \cdot 10^3$

Table 21. The total number of counts for the Ø 76.2 mm x 76.2 mm NaI(Tl) detector for different measurement geometries with the ^{133}Ba source from Table 6 placed in the radial centre of the barrel at "R0-A".

Geometry	**Total number of counts**
Stationary	$1.16 \cdot 10^5$
Rotating	$1.19 \cdot 10^5$

Figure 26 illustrates that there is a very small difference for when the ^{133}Ba source rotated and a slightly more pronounced difference for ^{57}Co. The difference is likely due to a radial displacement of the sources. The greater difference for ^{57}Co should be seen in relation to ^{133}Ba as they are two separate measurements but if there was a similar displacement the ^{57}Co have been more affected because of the greater sensitivity of lower energies for attenuation.

Table 20 and Table 21 support the discussion concerning Figure 26.

5.2.6 Sources placed at higher position

Figure 27 and Table 22 shows the results from the measurements where the source is placed at height 500 mm from the bottom of the barrel.

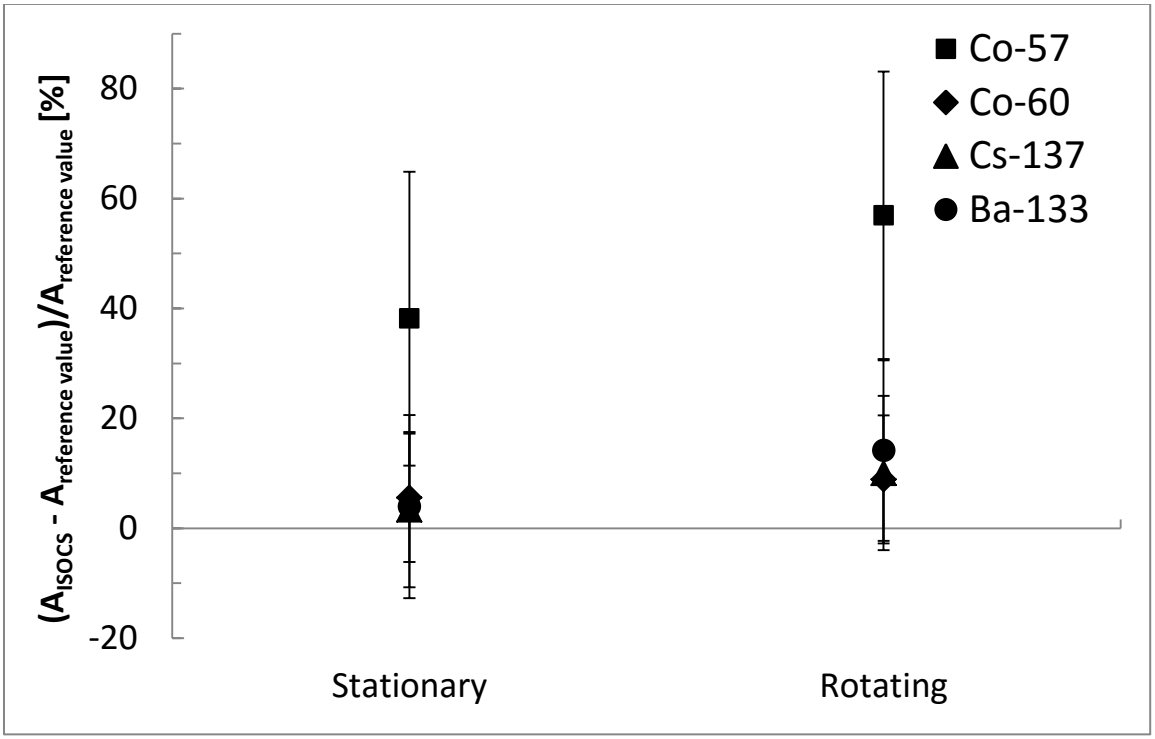

Figure 27. A graph over how much ISOCS™ activity estimation deviate from the reference activity for different measurement geometries where the point sources from Table 6 are placed higher up in the radial centre of the barrel at "R0-A".

Table 22. The total number of counts for the Ø 76.2 mm x 76.2 mm NaI(Tl) detector for different measurement geometries with the where the point sources from Table 6 are placed higher up in the radial centre of the barrel at "R0-A".

Geometry	Total number of counts
Stationary	$4.92 \cdot 10^5$
Rotating	$4.81 \cdot 10^5$

Figure 27 should be seen in relation to the "Rotating" value in Figure 23 which indicates that the activity estimation is higher when the sources are placed higher in the barrel meaning more in line with the detector. This is expected as more primary radiation will reach the detector but at the same time the software should be able to correct for the collimators. It seems that the software have difficulties with the lower energy lines of ^{57}Co. The slight difference between the stationary and rotating values is assumed to be caused by the same displacement of the sources in relation to the radial centre alternatively a displacement of the barrel on the rotating table or contributions from both.

Table 22 displays the opposite as the total number of counts is higher when the barrel was stationary. This cannot be explained by other means than displacement of the rotational centre of the barrel on the rotating table or that the NaI(Tl) detector is displaced in relation to the barrels rotational centre.

5.2.7 Final remarks

In general, setup 2 gave better results than setup 1. The variations decreased significantly and therefore it should be concluded that the aluminium rods affected the results. Variations still occurred but now it seems as they can be said to depend on faulty placement of the sources in the barrel or faulty placement of the barrel itself. The in general worse results for ^{57}Co are deemed to be caused by either that the software has difficulties at lower energies or that the source has too low activity. By reanalysing the spectra of ^{133}Ba for section1 in Figure 25 it is established that to achieve that underestimation a radial displacement of the source of 2 cm between the model and the measurement could explain the discrepancy. A radial displacement of 2 cm cannot be excluded thereby establishing this as the source of uncertainty for this setup. The overall conclusion is therefore that the system is very sensitive to the compliance between the modelled and the measured geometry. It is also suggested from a comparison between Figure 27 and Figure 23 that the system does not estimate the same activity if the sources are placed at a different vertical position in the barrel.

5.3 Relative measurements comparing different matrices using an ^{18}F liquid source

5.3.1 Water samples

Table 23 shows the analysis results from the water samples taken with two 200 ml beakers from the Radiometrics department at Studsvik after mixing ^{18}F with water.

Table 23. The analysis results after mixing ^{18}F with water. These results were obtained from the Radiometrics department at Studsvik Nuclear AB.

Beaker #	**Activity Concentration** [Bq/ml]
1	827
2	843

The values in Table 23 are to be considered having a dispersion around the mean of 2 % with no statistical uncertainty.

With the assumption that the barrel contained 100 litres of water based on a calculation of the volume of a cylinder with height 580 mm and radius 235 mm and an estimation of the weight of the barrel, both with and without water, the total content of ^{18}F in the barrel was 83.47 MBq.

5.3.2 ISOCS™

Table 24 shows the resulting estimated activity by ISOCS™ with different modelled and measured geometries at “R0-A”.

Table 24. The resulting estimated activity by ISOCS™ with different geometries with ^{18}F at "R0-A".

Modelled geometry	**Measurement geometry**	**Activity** [MBq]
Point source in radial centre	Point source in radial centre	94.35
Homogeneous activity distrib.	Point source in radial centre	35.67
Homogeneous activity distrib.	Point source in the radial periphery	84.26
Homogeneous activity distrib.	Homogeneous activity distribution	87.86

For this third setup the reference value is considered to be 83.47 MBq from the independent analysis and with this in mind the values in Table 24 shows that ISOCS™ will deviate by just below 60 % in the worst case scenario with a point source in the radial centre of the barrel when assuming homogeneous activity distribution. This is an important result as homogeneous activity distribution is always assumed in practice. ISOCS™ will have an overestimation by over 10 % when the source is modelled and measured in the radial centre with the barrel rotating. More importantly, the software will also give an overestimation when it is both modelled and measured homogeneously (circa 5 %) which is good from a radiological protection point of view.

From Table 23 it is clear that the content was indeed homogeneously distributed as these values are very close to one another and that they agree within the 2 % dispersion around the mean.

5.3.3 NaI(Tl) detector

Figure 28 below illustrates the total number of counts recorded with the NaI(Tl) detector as a function of the number of measurement for different measurement geometries.

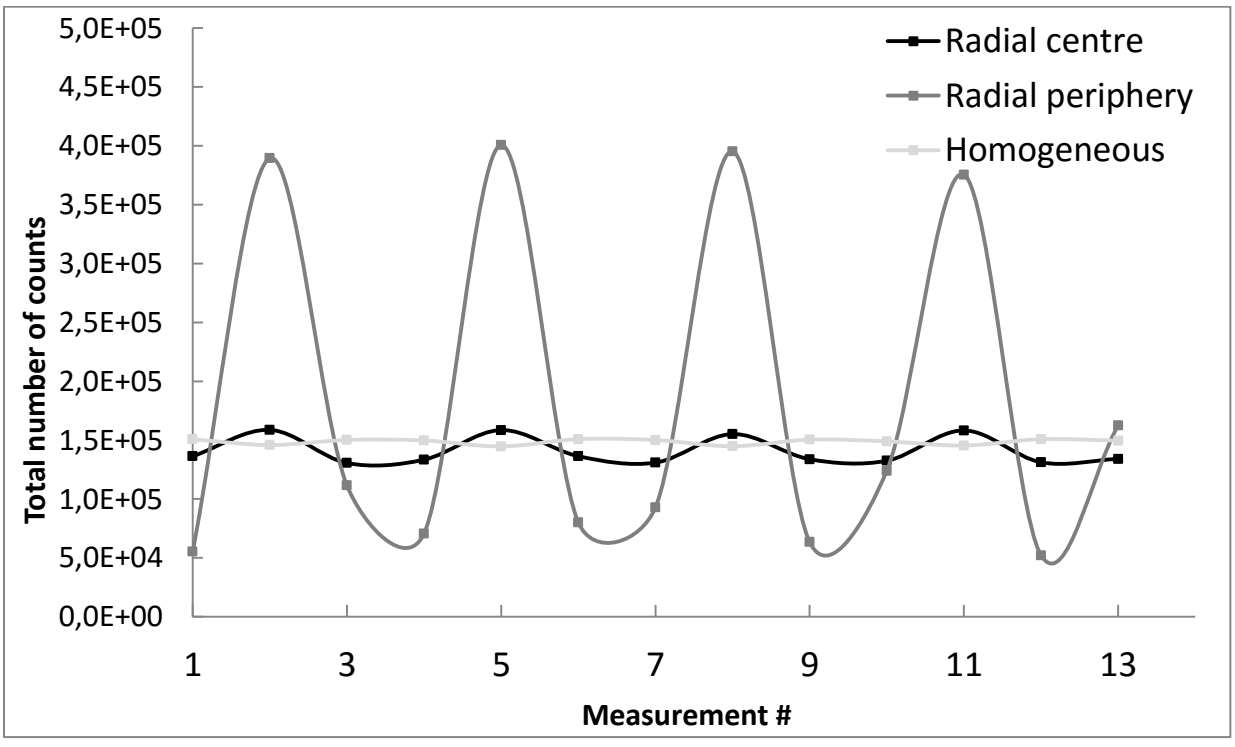

Figure 28. A plot over the variation of the total number of counts for the three different geometries used at the third setup collected with the Ø 76.2 mm x 76.2 mm NaI(Tl) detector at "R0-A". One measurement is equal to 5 seconds live time for the measurement with the source placed in the radial periphery whereas one measurement for the other two geometries are corrected with an assumed average real time of 6 seconds.

The key result for the work done to collect additional information is shown in Figure 28 as this shows that it is possible to assess the geometry by using a Ø 76.2 mm x 76.2 mm NaI(Tl) detector. The variations present in the figure for the homogeneous activity distribution and when the source was located in the radial centre indicate that the barrel was not centred on the rotating table alternatively that the NaI(Tl) detector was not aligned properly toward the rotational centre of the barrel. It is possible to see if there is a point source located at the radial periphery of the barrel. The unfortunate aspect of this figure is that no measurement was performed with the point source between the radial centre and the radial periphery.

By using a NaI(Tl) as used for this setup, it is possible to apply an estimation of the measurement uncertainty to a result obtained with ISOCS™. Should the NaI(Tl) detector show a factor 8 between the maximum and minimum value as in Figure 28 the estimated activity can be deemed to correspond well with the true activity content, as only a difference of 4 % is achieved between this case and the case of homogeneous activity distribution in Table 24. If instead a small variation or indeed no variation at all is obtained with the NaI(Tl) detector there is either homogeneous activity distribution or a point source in the radial centre. These cases will differ because if the content is homogeneously distributed the estimated activity can be assumed to correspond with the true activity content in the waste. Should there instead be a point source in the radial centre of the barrel the estimated activity will be 60 % too low. So to distinguish between these two cases the NaI(Tl) detector can be moved closer to the barrel. If the content is homogeneously distributed the $1/r^2$ dependency will *not* be valid, but if the content is located in a point source the $1/r^2$ dependency *will* be valid and 60 % can thus be added to the estimated activity.

5.3.4 Weighting of radial position

The assumed linear dependency from section 3.2 between the two extreme values in Table 24 is presented in Figure 29 and the relative weighting factor as function of the radial position of the point source is presented in Figure 30.

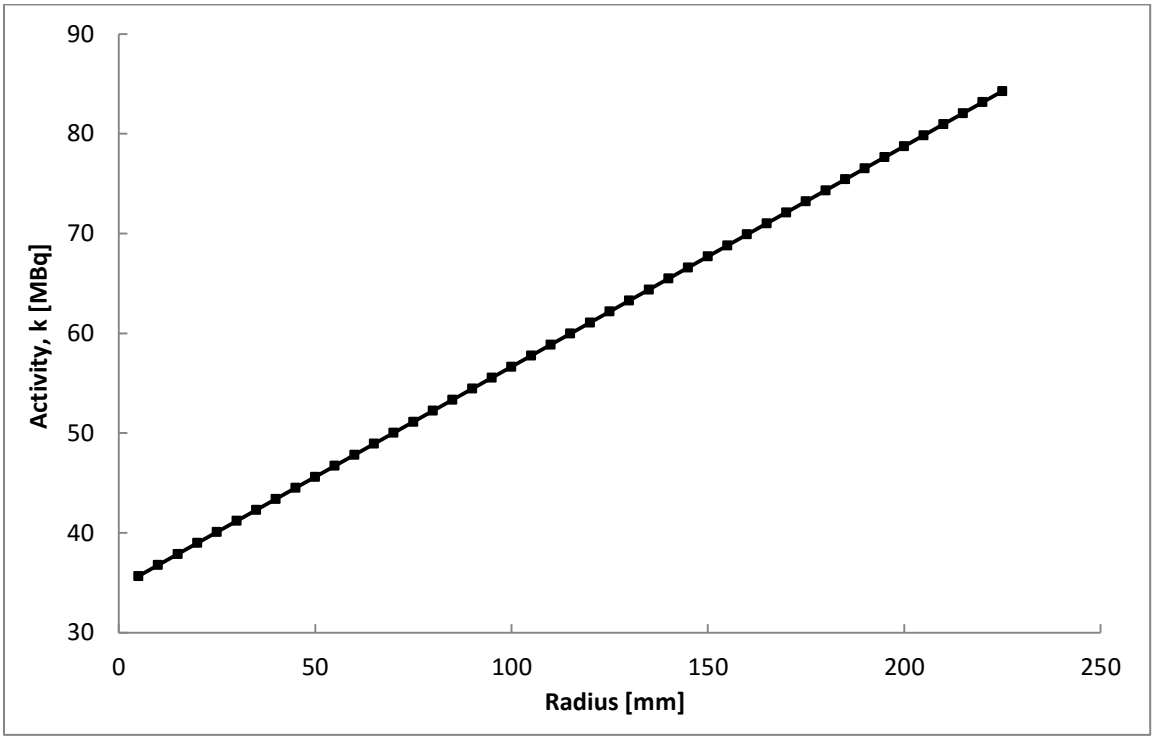

Figure 29. A graphic representation of the assumed linear dependency of how the activity estimate by the Genie™ and ISOCS™ software change when a point source with radius 5 mm is moved from barrel radius 5 mm to 225mm.

The linear dependence between the radial positions of the point source in Figure 29 is assumed in lack of better evidence. Here as well it is unfortunate that no measurement was performed with the source placed between the extremes. If it had been performed the linear dependency could have been either confirmed or disowned.

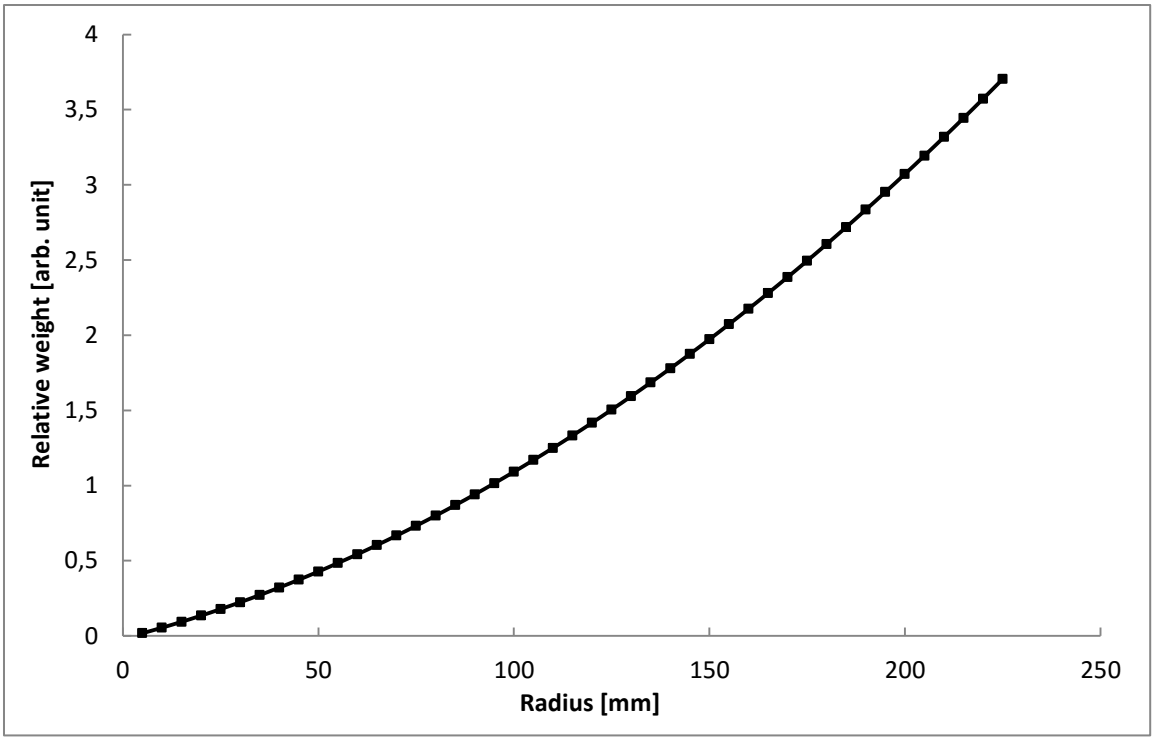

Figure 30. A graphic representation of how the relative weight depend on which radius a point source with radius 5 mm is placed in a barrel. Each step in the curve represents a cylindrical volume element with a radius 5 mm greater than the last element.

Figure 30 shows that the maximum weighting factor that can be achieved is just below 4 when a 10 mm point source is located at 225 mm from the radial centre. The figure also shows that the weighting factor increases exponentially with radial position of the source.

5.3.5 Final remarks

The difference in activity estimation for ISOCS™ between the worst and best case scenario is an underestimation of roughly 60 %. A Ø 76.2 mm x 76.2 mm NaI(Tl) detector can be used to assess the position of a point source if it is located in the radial periphery of a barrel or the radial centre of a barrel or if the content is homogeneously distributed. No measurement was performed with the source placed between the radial centre and the periphery which could have affected the assumed linear dependency for the activity estimation as a function of radial position of a point source with diameter 10 mm. The relative weight of the location of a point source is exponential and the maximum weighting factor is just below 4 for when a point source is located 225 mm from the radial centre.

5.4 Measurements to estimate reproducibility

For the first geometry the maximum difference between the total number of counts recorded with the Ø 76.2 mm x 76.2 mm NaI(Tl) detector was 1.86 %. For the second geometry the maximum difference between the total number of counts recorded with the Ø 76.2 mm x 76.2 mm NaI(Tl) detector was 0.93 %.

The results from these estimations indicate that repeating the same measurement will not affect the result in a significant way. This of course depends upon what accuracy is wanted or needed. But seen in relation to the deviations from the first two sets of measurement just under 2 % reproducibility cannot be regarded as affecting the overall view of the system and its accuracy.

6 Conclusions

This work has examined how well Canberra's ISOCS™ estimated the activity content in a waste barrel with different radionuclide content and waste matrices. The measurements performed have shown that the activity content can be well estimated when the content is homogeneously distributed and does not contain radionuclides with low energy photons. The deviation from the reference value generally reduces as the photon energy increases thereby indicating that the higher the energies the less conservative the system is in estimating the activity. The system has difficulties when the waste matrix is more complex and the content has a wide array of photon energies. For those cases the difference between the estimated activity and the activity of the reference sources is larger. However, the software cannot entirely be to blame as it is practically impossible to model the exact geometry as there are limitations primarily in the setup of measurements. Therefore it is difficult to claim anything else than that ISOCS™ estimates the content well when the modelled geometry has very good correspondence with the measured geometry and to conclude that the program is sensitive for discrepancies between model and reality. It also seems that ISOCS™ has difficulty when it comes to assessing radionuclides with low energies independent of the waste matrix.

This work was also set out to estimate the accuracy for the estimated activity. Measurements performed indicate that ISOCS™ can in the worst case scenario with a point source placed in the radial centre of a barrel filled with water underestimate the activity content by 60 % for ^{18}F. Thus with an addition of 60 % to the estimated activity from a measurement assuming homogeneous activity distribution, the user is always safe that the activity from radionuclides with higher photon energies than ^{18}F, such as ^{137}Cs and ^{60}Co, will be within this uncertainty of 60 %. This is true under the condition that the density for the surrounding material is 1 g/cm³ and that it is homogeneously distributed. In addition to this a few percent can be added for reproducibility for a similar setup.

A Ø 76.2 mm x 76.2 mm NaI(Tl) detector can be used as a tool to gain additional information regarding the activity distribution in the barrel and can with ease be used to determine if an inhomogeneity in the form of e.g. a point source is located far from the radial centre of a rotating barrel. The additional detector information can also be used to determine the accuracy for the activity estimation when a homogeneous activity distribution is assumed but not known in practice.

7 References

1. International Atomic Energy Agency (2007). *Strategy and Methodology for Radioactive Waste Characterization.* IAEA-TECDOC-1537. Vienna: IAEA. ISBN 92-0-100207-6.

2. International Atomic Energy Agency (1998). *Radiological Characterization of Shut Down Nuclear Reactors for Decommissioning Purposes.* IAEA Technical Report Series no. 389. Vienna: IAEA. ISBN 92-0-103198-X.

3. International Atomic Energy Agency (2009). *Determination and Use of Scaling Factors for Waste Characterization in Nuclear Power Plants.* IAEA Nuclear Energy Series No. NW-T-1.18. Vienna: IAEA. ISBN 978-92-0-110808-1.

4. Remeikis, V., Plukis, A., et al. (2009). Study of the nuclide inventory of operational radioactive waste for the RBMK-1500 reactor. *Nuclear Engineering and Design*. 239 (4), 813-818.

5. Canberra Industries Inc. (2013). *Model S573 In Situ Object Counting System (ISOCS™) Calibration Software Data Sheet.* Available: http://www.canberra.com/products/insitu_systems/pdf/ISOCS-SS-C40166.pdf. Last accessed: April 21 2015.

6. ORTEC® (2014). *ISOTOPIC software brochure*. Available: http://www.**ortec**-online.com/download/**ISOTOPIC**.pdf . *Last accessed: April 21 2015.*

7. Kalb, P., Luckett, L., Miller, K., Gogolak, C. and Milian, L. (2000). *Comparability of ISOCS instrument in radionuclide characterization at Brookhaven National Laboratory.* Formal Report BNL-52607. New York: BNL.

8. Dewberry, R.A., Casella, V.R., et al. (2009). Benchmarking Ortec ISOTOPIC measurements and calculations. *Journal of Radioanalytical and Nuclear Chemistry.* 281(3), 313-321.

9. Slaninka, A., Slávik, O. and Nečas, V. (2010). Uncertainty analysis of in-situ gamma spectrometry measurements of air cleaning filter cartridges and 200 L barrels by a HPGe detector. *Applied Radiation and Isotopes.* 68 (7-8), 1273-1277.

10. Saltykov, L.S., Shevchenko, S.V., et al. (2010). Impact of heterogeneity on Gamma-Spectrometry Data at Nondestructive Assay of Radioactive Waste. *Practice Periodical of Hazardous, Toxic, and Radioactive Waste Management.* 14 (3), 205-210.

11. Dean, J. (2009). A UK comparison for measurements of low levels of gamma-emitters in waste barrels. *Applied Radiation and Isotopes.* 67(5), 678-682.

12. Miller, K.M., Shebell, P., Monetti, M.A., et al. (1998). An Intercomparison of In Situ Gamma-Ray Spectrometers. *Radioactivity and Radiochemistry*. 9 (4), 27-40.

13. Hong, S.B., Seo, B.K., et al. (2005). *A comparison of the experimental and ISOCS gamma spectrometric methods for activated concrete samples*. Proceedings of the KNS spring meeting, Jeju, South Korea 26-27 May 2005.

14. Sansone, K.R. (2013). *MIRCOSHIELD/ISOCS Gamma Modeling Comparison.* Sandia Report SAND 2013-6475. United States of America: Sandia National Laboratories.

15. Dean, J. (2013). *NPL Nuclear Industry Proficiency Test Exercise 2012.* NPL Report IR 30. Middlesex: National Physics Laboratory. ISSN 1754-2952.

16. Hung, P-J., Chiu, H-S., et al. (2012). The performance evaluation of a movable gamma-ray counting system for radwaste measurement. *Applied Radiation and Isotopes.* 70 (9), 1977-1980.

17. Carbonez, P., La Torre, F.P., et al. (2012). Residual radioactivity at the CERN 600 MeV synchro-cyclotron. *Nuclear Instruments and Methods in Physics Research.* 694, 234-245.

18. Bergman, C. (2009). *Kartläggning av fast avfall innehållande radioaktiva ämnen från icke kärntekniska verksamheter – sammanställning av tidigare rapporter.* Report number 2009:23. Stockholm: Swedish Radiation Safety Authority. ISSN 2000-0456.

19. International Atomic Energy Agency (2009). *Classification of Radioactive Waste.* General Safety Guide No. GSG-1. Vienna: IAEA. ISBN 978-92-0-109209-0.

20. Government Offices of Sweden and Ministry of the Environment Sweden (2014). *Sweden's fifth national report under the Joint Convention on the safety of spent fuel management and on the safety of radioactive waste management: Sweden's implementation of the obligations of the Joint Convention*. Swedish Government Official Reports and the Ministry Publications Series Ds 2014:32. ISBN 978-91-38-24168-4.

21. International Atomic Energy Agency (2011). *Disposal of Radioactive Waste.* Specific Safety Requirements No. SSR-5. Vienna: IAEA. ISBN 978-92-0-103010-8.

22. International Commission on Radiological Protection (2007). *2007 Recommendations of the International Commission of Radiological Protection – Annals of the ICRP, ICRP Publication 103.* Volume 37. Elsevier. ISBN 978-0-7020-3048-2.

23. International Atomic Energy Agency (2003). *Radioactive Waste Management Glossary – 2003 Edition.* Vienna: IAEA. ISBN 92-0-105303-7.

24. International Atomic Energy Agency (2004). *Application of the Concepts of Exclusion, Exemption and Clearance.* Safety Guide No. RS-G-1.7. Vienna: IAEA. ISBN 92-0-109404-3.

25. Swedish Radiation Safety Authority (2011). *Strålsäkerhetsmyndighetens föreskrifter och allmänna råd om friklassning av material, lokaler, byggnader och mark vid verksamhet med joniserande strålning.* Report number 2011:2. Stockholm: Swedish Radiation Safety Authority. ISSN 2000-0987.

26. European Commission (2000). *Radiation protection 122 - Practical Use of the Concepts of Clearance and Exemption, part I: Guidance on General Clearance Levels for Practices.* EU: European Commission.

27. Svensk Kärnbränslehantering AB (2011). *Kärntekniska industrins praxis för friklassning av material, lokaler och byggnader samt mark.* SKB Report number R-11-15. ISSN 1402-3091.

28. Bücherl, T., Kaciniel, E. and Lierse, Ch. (1998). *Synopsis of Gamma Scanning Systems: Comparison of Gamma Determining Systems and Measuring Procedures for Radioactive Waste Packages.* European Network of Testing Facilities for the Quality Checking of Radioactive Waste Packages, European Commission Report WG-A-01.

29. Filβ, P. (1995). Relation Between the Activity of a High-Density Waste Barrel and its Gamma Count Rate Measured With an Unshielded Ge-detector. *Applied Radiation and Isotopes.* 46 (8), 805-812.

30. Dung, T.Q. (1997). Calculation of the systematic error and correction factors in gamma waste assay systems. *Annals of Nuclear Energy.* 24 (1), 33–47.

31. Bai, Y.F., Mauerhofer, E. et al.. (2009). An improved method for the non-destructive characterization of radioactive waste by gamma scanning. *Applied Radiation and Isotopes*. 67 (10), 1897-1903.

32. Krings, T., Mauerhofer, E. (2010). Reconstruction of the activity of point sources for the accurate characterization of nuclear waste barrels by segmented gamma scanning. *Applied Radiation and Isotopes*. 69 (6), 880-889.

33. Krings, T., Mauerhofer, E. (2012). Reconstruction of the isotope activity content of heterogeneous nuclear waste barrels. *Applied Radiation and Isotopes*. 70 (7), 1100-1103.

34. Krings, T., Genreith, C. et al. (2013). A numerical method to improve the reconstruction of the activity content in homogenous radioactive waste barrels. *Nuclear Instruments and Methods in Physics Research*. 701, 262-267.

35. Savidou, A., Tzika F. and Stamatelatos, I. (2007). *Characterization of radioactive waste barrels by non destructive gamma spectrometry*. 4th International Conference on NDT, Chania, Greece 11-14 October 2007.

36. Dinescu, L., Vata, I.L., et al. (2002). On the efficiency calibration of a barrel waste assay system. *Nuclear Instruments and Methods in Physics Research*. 487 (3), 661-666.

37. Yuan, M-C., Yeh, C-H., et al. (2009). The calibration and evaluation of a radioactive waste barrel counting system. *Applied Radiation and Isotopes*. 67 (5), 931-934.

38. Yuan, M-C., Yeh, C-H., et al. (2010). Proficiency testing feasibility study for the measurement of gamma-emitting clearance samples. *Applied Radiation and Isotopes*. 68 (7-8), 1211-1216.

39. Yeh, C-H., Yuan, M-C., et al. (2012). Proficiency testing for clearance mixed-nuclide samples. *Applied Radiation and Isotopes*. 70 (9), 1856-1859.

40. Canberra Industries, Inc. (2013). *ISOCS/LabSOCS Detector Characterization Report – Detector Model GC4018*. United States of America: Canberra Industries, Inc.

41. Breismeister, J.F. (ed.) (March 2000). *MCNP – A general Monte Carlo N Particle Transport Code Version 4C*. Los Alamos National Laboratory Report LA-13709-M.

42. AMETEK®. *ORTEC® digiBASE™: 14-pin PMT Rod Base with Integrated Bias Supply, Preamplifier, and MCA (with Digital Signal Processing) for NaI Spectroscopy.* Available: www.ortec-online.com/download/digiBASE.pdf. Last accessed: April 14 2015.

43. IAEA (2015). *Livechart – Table of Nuclides – Nuclear structure and decay data*. Available: https://www-nds.iaea.org/relnsd/vcharthtml/VChartHTML.html. Last accessed April 14 2015.

44. Capintec Inc. (2003). *CRC®-35R Radioisotope dose calibrator owner's manual.* Manual Stock no. 9250-0054. Available: http://www.capintec.com/?ddownload=893. Last accessed: May 21 2015.

45. Canberra Industries, Inc. (2009). *Genie™ 2000 Spectroscopy Software – Customization Tools.* United States of America: Canberra Industries, Inc. ICN 9233653G V3.2.

46. Venkataraman, K, Bronson, F. et al.. (2005). Improved detector response characterization method in ISOCS and LabSOCS. *Journal of Radioanalytical and Nuclear Chemistry*. 264 (1), 213-219.

47. Canberra Industries Inc. (2013). *Genie™ Basic Spectroscopy Software Data Sheet*. Available: http://www.canberra.com/products/radiochemistry_lab/pdf/G2K-BasicSpect-SS-C40220.pdf. Last accessed: April 29 2015.

48. Canberra Industries Inc. (2013). *Genie™ Gamma Analysis Software Data Sheet*. Available: http://www.canberra.com/products/radiochemistry_lab/pdf/Gamma-Analysis-SS-C40221.pdf. Last accessed: April 29 2015.

49. Canberra Industries Inc. (2008). *Genie™ Quality Assurance Software Data Sheet*. Available: http://www.canberra.com/products/radiochemistry_lab/pdf/IPF-C37116.pdf. Last accessed: April 29 2015.

50. Canberra Industries Inc. (2009). *Genie™ Interactive Peak Fit Data Sheet*. Available: http://www.canberra.com/products/radiochemistry_lab/pdf/IPF-C37116.pdf. Last accessed: April 29 2015.

51. Canberra Industries Inc. (2011). *Apex-Gamma™Lab Productivity Suite Data Sheet*. Available: http://www.canberra.com/products/radiochemistry_lab/pdf/Apex-Gamma-C39240.pdf. Last accessed: April 29 2015.

52. AMETEK®. *ORTEC® MAESTRO®-32 V6: Powerful MCA Emulation Software.* Available: http://sites.fas.harvard.edu/~phys191r/Bench_Notes/A5/maestro_brochure.pdf. Last accessed: April 29 2015.

Appendix A

A.1 Generating and validating the detector characterization file

Generating a detector characterization file involves several steps. The first step in producing a so called Detector Calibration Grid (DCG) file is by sorting the crystal efficiencies by their value of θ and then by their value of Ln(R). Then, using a cubic spline interpolation, the efficiencies at a large number of nodal points are generated via interpolation of the bare-crystal reference data. In doing this, the DCG process creates a spatially dense grid of efficiencies at each of the 20 photon energies in the Ln(R)-θ coordinate system. By then using ISOCS™ based algorithms the attenuation due to the external crystal structures are computed for each point once the full grid of energies are created. The now attenuated efficiency grids are then combined, thus producing the ISOCS™ detector characterization. Obtaining the efficiency at any arbitrary spatial point between the grid nodes is done by linear interpolation along the Ln(R) and θ directions whereas the efficiency at any arbitrary energy (between 10 keV and 7000 keV) is obtained by parabolic interpolation between the energy grids.

Because of the geometry of the detector, its efficiency response is cylindrically symmetric about its axis. Hence, the response characterization that is valid within a semi-circular plane of a given radius is valid within a hemispherical region about the detectors symmetry axis as well. So, the ISOCS™ characterization can be said to represent the response of the detector to a point source in vacuum anywhere within a sphere with a 500 m radius and centred about the detector, at any energy in the interval 10-7000 keV. Given the DCG'-s and taking the attenuation through the materials in the geometry into account, the ISOCS™ software can calculate the efficiency for macroscopic sources by integrating the response over the active volume (or volumes) of a given geometry.

The DCG is validated in two steps[46]; a statistical test to validate the quality of the DCG grids and a validation of DCG efficiencies using measurements. The statistical test is performed in order to check the interpolation quality of the bare-crystal DCG grids by generating secondary sets of point source locations, intermediate to the primary set of points. The efficiencies for these secondary points are then determined by linear interpolation using the primary DCG grids. By using the efficiencies at the intermediate points, a secondary set of DCG grids is created. From these secondary DCG grids the efficiencies at the primary point locations are acquired and compared to the MCNP efficiencies at the primary points. Hence, a relative deviation of the grid efficiencies with respect to the MCNP efficiencies can be given, as well as the standard deviation of it, within a specified spatial region. For efficiency points within a DCG region at the various photon energies where the DCG grids have been created, five pieces of statistics are reported; i.) the percentage average relative deviation of the second DCG efficiencies with respect to the MCNP efficiencies, ii.) the percentage standard deviation in these relative deviations, iii.) the percentage standard deviation of the MCNP data averaged over the number of points in the DCG region, iv.) the number off efficiency data points within 1σ, between 2σ and 3σ, and between 2σ and 3σ confidence intervals, at the various DCG energies and lastly v.) the number of data points located outside the 3σ limit. These pieces of statistic are acquired for six pre-defined spatial regions deemed most likely for sample location for in-situ as well as laboratory users. The relative deviations and the standard deviations are computed only for the data points that are within these spatial regions, and are meant to provide information regarding the quality of the response characterization within these particular regions.

To be able to compare with measurements the file containing the DCG grid is loaded into ISOCS™ software and generates efficiencies for the 0°, 90° and 135° point source geometries and for the PMMA mounted source geometries.

Appendix B

B.1 Modelling measurement geometries

In order to perform an efficiency calibration the different measurement geometries had to be modelled. This was achieved with Geometry Composer v. 4.2.1 which is a program included in the Genie™ 2000 Gamma Analysis software (see section 4.5). In Geometry Composer there are different templates from which to specify the geometry used. For all the performed measurements the template "Simple Cylinder", "Complex Cylinder" or "Sphere" was used as shown in Figure B1, Figure B2 and Figure B3, respectively.

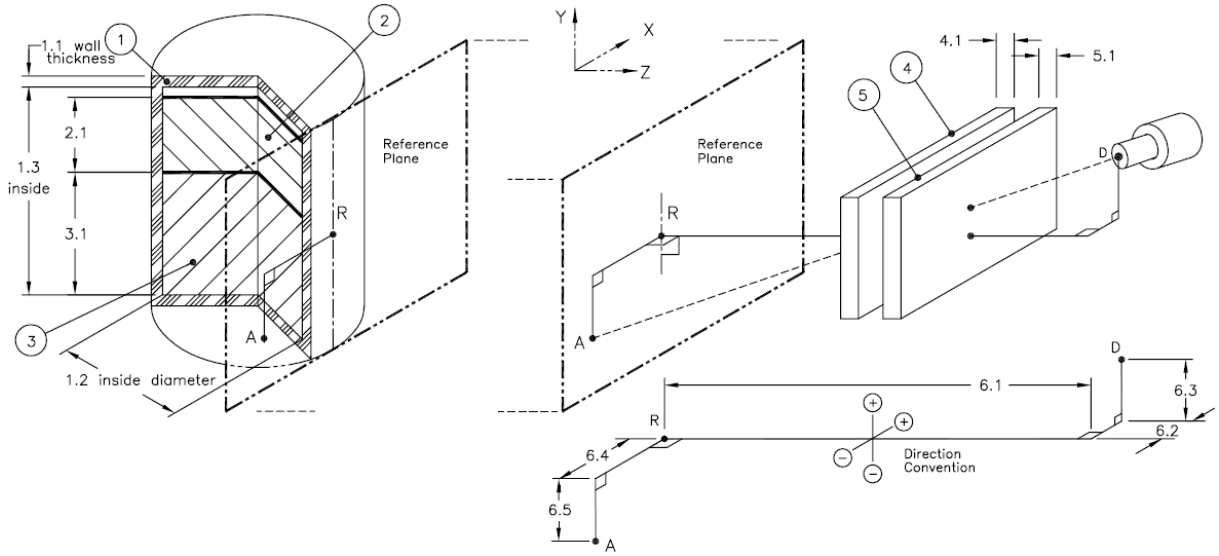

Figure B1. The template "Simple Cylinder". In the template, R is the source reference point, i.e. the centre of line where the plane contacts the cylinder. D is the detector reference point in form of the centre of the end cap. A is the detector aiming point and is anywhere on the reference plane. For description of the different numbers, see text.

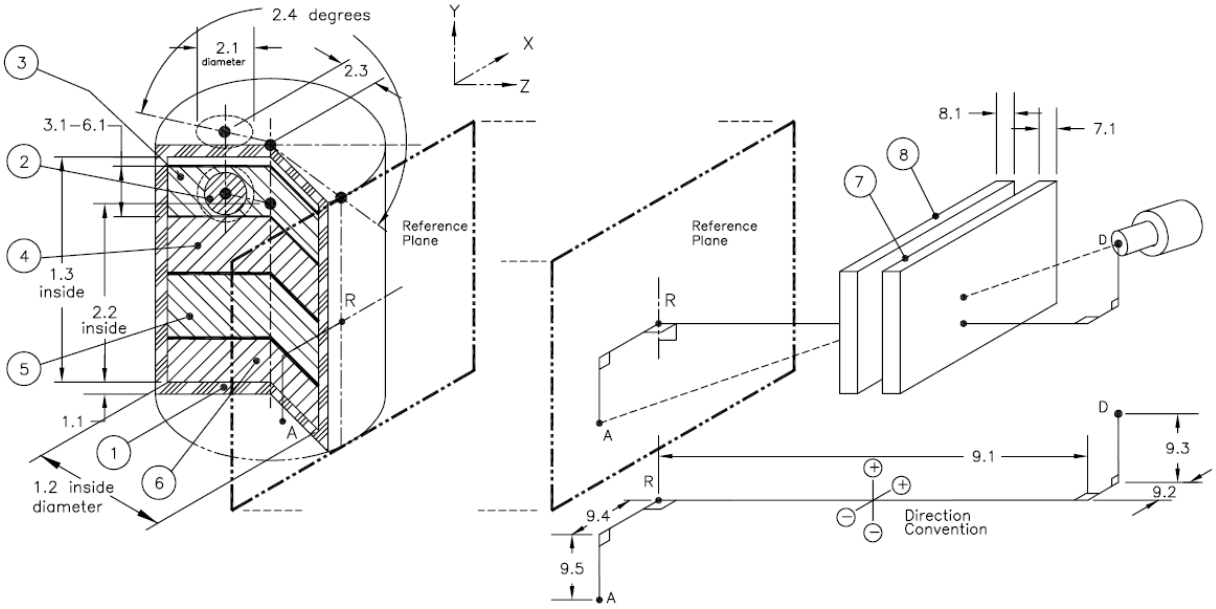

Figure B2. The template "Complex Cylinder". In the template, R is the source reference point, i.e. the centre of line where the plane contacts the cylinder. D is the detector reference point in form of the centre of the end cap. A is the detector aiming point and is anywhere on the reference plane. For description of the different numbers, see text.

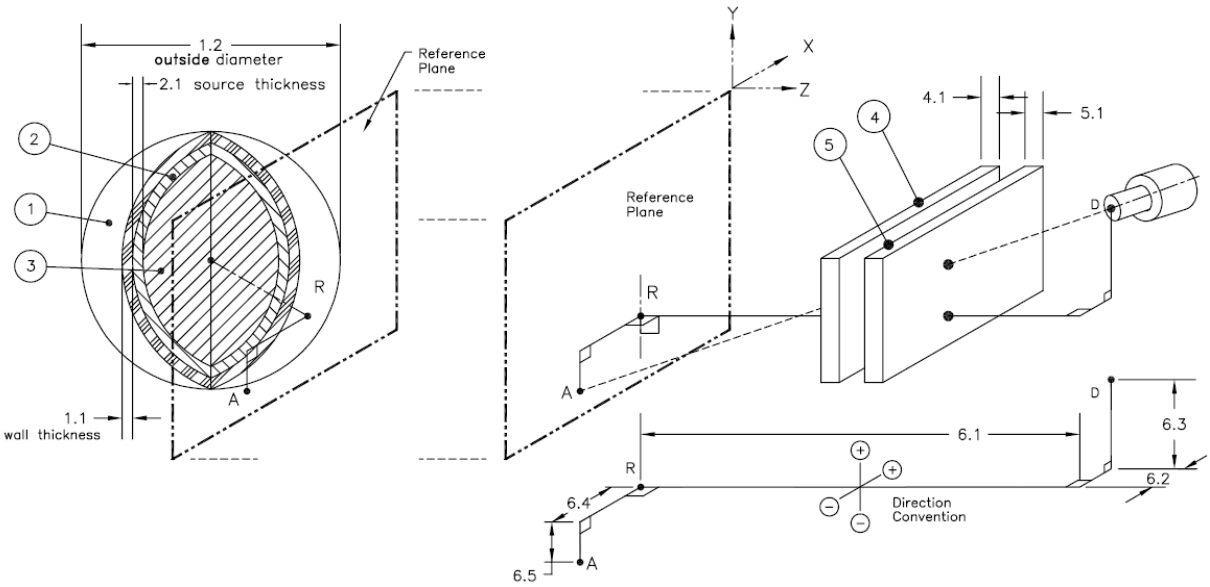

Figure B3. The template "Sphere". In the template, R is the source reference point, i.e. the centre of line where the plane contacts the cylinder. D is the detector reference point in form of the centre of the end cap. A is the detector aiming point and is anywhere on the reference plane. For description of the different numbers, see text.

For the "Simple Cylinder" template item number 1 denotes the dimensions of the cylinder (barrel) where the inside height, inside diameter and wall thickness are defined. Item number 2 and 3 denotes the height of the bottom and eventual top layer of the source. Item number 4 and 5 denotes the thickness of any 2 eventual absorbers between the detector and the reference plane. Item number 6 denotes different dimensions relating the detector to the source, including distance and offset in the x-, y- and z-direction. For all item numbers except for item number 6 the template requires the material and density of that item number if it is defined. For item number 2 and 3 the template also requires the relative concentration of the source.

For the "Complex Cylinder" template item number 1 denotes the dimensions of the cylinder where the inside height, inside diameter and wall thickness are defined. Item number 2 denotes the diameter of the source, its height from the bottom of the cylinder, its distance from the radial centre of the cylinder and the angle of the source in relation to the reference plane. Item number 3, 4, 5 and 6 denotes the height of four different layers of content from top to bottom. Item number 7 and 8 denotes the thickness of any 2 eventual absorbers between the detector and the reference plane and item number 9 denotes different dimensions relating the detector to the source, including distance and offset in the x-, y- and z-direction. For all item numbers except for item number 9 the template requires the material and density of the item numbers if they are defined. For item numbers 2-6 the template also requires the relative concentration of the source.

In the "Sphere" template item number 1 denotes the wall thickness and outside diameter of the spheres shell. Item number 2 denotes the thickness of the shell of the source whereas item number 3 only the material of the source and its density need be defined. Item number 4 and 5 denotes the thickness of any 2 eventual absorbers between the detector and the reference plane. Item number 6 denotes different dimensions relating the detector to the source, including distance and offset in the x-, y- and z-direction. For all item numbers except for item number 6 the template requires the material and density of that item number. For item number 2 and 3 the template also requires the relative concentration of the source.

Appendix C

C.1 Software

The two different ISOCS™ systems both utilises software from Canberra in order to model the measurement geometries, perform calibration and analyse the resulting data. The software in question is presented in Table C1.

Table C1. The software used in order to model measurement geometries, perform calibration and analyse the resulting data[47,48,49,50,5].

Software	Version
Genie™ 2000 Basic Spectroscopy	3.2.1
Genie™ 2000 Gamma Analysis	3.2.3
Genie™ 2000 Quality Assurance	1.3
Genie™ 2000 Interactive Peak Fit	1.3.1
ISOCS™ Calibration Software	4.2.1

The software in Table C1 is integrated in Apex-Gamma™ Lab Productivity Suite v. 1.3[51]. The same software except for Apex-Gamma™ was used to reanalyse the data if and where this were needed. When using these software Apex-Gamma™/ ISOCS™ gives an uncertainty for the estimated activity which is based on counting statistics in the photo peaks (Apex-Gamma™) and the efficiency calibration (ISOCS™).

The NaI(Tl)-detector system were connected with a USB-cable to a laptop that contained the software MAESTRO-32 for Windows Model A65-B32 version 6.03[52] which collected the spectra from the detector.